Comparing lodgepole pine defence responses against mountain pine beetle and *Grosmannia clavigera*

by

Duowen Pu

A thesis submitted in partial fulfillment of the requirements for the degree of

Master of Science

in

Plant Biology

Department of Biological Sciences
University of Alberta

Abstract

The mountain pine beetle (*Dendroctonus ponderosae* Hopkins; MPB) is a bark beetle that poses a significant threat to pine species in western North America. This threat is evident in the ongoing MPB epidemic, which has resulted in significant losses of lodgepole pine (*Pinus contorta* var. *latifolia*) forests. One reason for the effectiveness of MPB attacks on lodgepole pine is their symbiotic relationship with ophiostomatoid fungal associates like *Grosmannia clavigera* (Robinson-Jeffrey and Davidson) Zipfel, de Beer and Wingfield. Recent research used plant defense hormone profiling to cast doubt on the contribution that *G. clavigera*, makes to MPB's capacity to overcome lodgepole pine defenses during mass attack. These analyses showed that *G. clavigera*-inoculated lodgepole pine synthesize significantly increased levels of jasmonate (JA) and the active conjugate jasmonate-isoleucine (JA-Ile) as well as the ethylene (ET) precursor 1-aminocyclopropane-1-carboxylate (ACC). JA and ET are the hormone signature of plant response to necrotrophic fungal pathogens. In contrast, lodgepole pine trees subjected to MPB mass attack exhibited significantly increased levels of JA and JA-Ile but not ACC during the mass attack phase, as expected for plant responses to herbivore insects. The lack of ACC synthesis in lodgepole pines during the mass attack phase suggests that ophiostomatoid fungal symbionts have not begun to colonize host tissues during mass attack, and as such do not contribute to MPB's capacity to overcome lodgepole pine defenses during this critical phase of insect-host interactions. Building upon this recent study, my study investigated expression patterns of jasmonic acid (JA) and ethylene (ET) biosynthesis and signaling genes in MPB-attacked versus *G. clavigera*-inoculated lodgepole pines. I hypothesized that if *G. clavigera* does not significantly contribute to MPB's capacity to overcome tree defenses, the tree's response to MPB during the mass attack phase would involve JA biosynthesis and

signaling genes but not ET biosynthesis and signaling genes. Since increased expression of genes coding for biosynthetic enzymes often precedes increased levels of their metabolite products, analyzing transcript abundance profiles for JA and ET biosynthesis genes enabled me to explore potential roles for JA and ET in lodgepole pine's response to MPB during the transition from mass attack to colonization. Based on previous transcriptome profiling experiments, I identified, cloned and carried out *in silico* analyses of six lodgepole pine cDNAs putatively involved in JA- and ET-mediated responses : lipoxygenase (*PcLOX)* and allene oxide synthase (*PcAOS*) for JA biosynthesis, jasmonate ZIM-domain (*PcJAZ)* for JA signaling, and 1-aminocyclopropane-1-carboxylate oxidase (*PcACO1* and *PcACO2*) and 1-aminocyclopropane-1-carboxylic acid synthase (*PcACS*) for ET biosynthesis. I then carried out transcript abundance profiling by quantitative reverse transcriptase polymerase chain reaction (qRT-PCR) in secondary xylem and secondary phloem harvested from mature lodgepole pine trees that were either mass attacked by MPB or inoculated with *G. clavigera*, comparing these treatments with both unwounded controls and mock-attacked or mock-inoculated controls. JA-related genes *PcLOX* and *PcJAZ* showed significant upregulation in MPB-attacked, *G. clavigera*-inoculated and mock-treated trees, consistent with the model that chewing herbivorous insects, necrotrophic fungal pathogens and mechanical wounding all trigger the JA pathway. I observed significant upregulation of ET biosynthesis genes *PcACO1* and *PcACO2* following *G. clavigera* inoculation, and in in response to wounding and MPB attack. These significant increases in *PcACO1* and *PcACO2*gene expression mirrored measured ACC levels in *G. clavigera*-inoculated trees, but not in mock- or MPB-attacked samples. The increases in *PcACO1* and *PcACO2*gene transcript abundance in MPB-attacked trees, which were only measured at the later time point and not earlier time point, could be interpreted to mean that *G. clavigera* colonization was

sufficient to trigger plant perception of the fungal pathogen during the transition from mass attack to colonization, but that increased ET biosynthesis gene expression had not yet translated into increased ACC levels. Alternatively – or additionally –increased expression of ET biosynthesis genes may have been associated with production of traumatic resin ducts, a classic response of conifer species to wounding, herbivore and pathogen attack. ET has also been recently implicated in plant repair responses. These transcript profiling experiments reveal an additional layer of complexity in the roles for ET in host responses to MPB attack that require additional experiments to resolve.

Preface

Plant materials that I analyzed in my thesis were from an experiment conducted by Dr. Colleen Fortier and Dr. Antonia Musso. Dr. Colleen Fortier together with Dr. Irina Zaharia carried out the plant hormone profiling experiment that formed the foundation of my thesis. Houtan Vafaeifard contributed to identification of target gene *PcJAZ*, I conducted the identification of other target genes, based on a microarray experiment analysis carried out by members of the Cooke Lab. RNA extraction was conducted with the assistance from Marion Mayerhofer. The design of qRT-PCR primers was accomplished with guidance from Troy Locke. I performed the statistical analyses with the support of Samson Osadolor and Dr. Colleen Fortier. This collective effort has greatly contributed to the integrity and depth of the research presented herein.

Acknowledgements

I humbly recognize that the area in which I live and study falls within Treaty 6 territories, ancestral lands of the First Nations and Métis peoples. I acknowledge that the privilege has allowed me to inhabit these lands and benefit from the stewardship of indigenous communities.

I would like to thank my supervisor, Dr. Janice Cooke, who gave me the opportunity to conduct this research in her lab. After completing my bachelor's degree, I was uncertain about my academic ideals and career development, especially with the challenges brought on by the arrival of Covid-19. The precious opportunity from Janice provided me a clear direction and allowed me to pursue my passion in Biology. Furthermore, her encouragement, invaluable support and constructive guidance have been helpful in shaping this study and my growth as a researcher. I am deeply grateful for the opportunity to work under her supervision, and I acknowledge her significant contributions to the success of this project.

I would like to thank the member of my supervisory committee, Dr. Guanqun (Gavin) Chen, for his invaluable contributions in shaping my research aspirations. I would like to thank the entire Cooke lab team, particularly Dr. Colleen Fortier, Marion Mayerhofer and Samson Osadolor. In my first year in Canada, I struggled to use English, my second language, to participate in my work and adapt to a new environment. However, they showed great patience in guiding and assisting me, and have become my dear friends, enriching this academic endeavor beyond measure. Thank you to all the staff of the Department of Biological Sciences, particularly Troy Locke, whose support has been instrumental in elevating the quality of this research.

I express my appreciation for all the financial support I have received, enabling me to devote my most effort to this thesis. This support includes funding from the Department of Biological Sciences and MITACS.

Thank you to all my friends and family for their love, encouragement and understanding throughout the duration of this program. Thank you to my love, Junlong, for being my only family in a foreign land. You treat me with love, honesty, tenderness, and generosity, making Canada feel just like home to me.

Table of Contents

List of Tables

List of Figures

List of Abbreviation

ACC	1-aminocyclopropane-1-carboxylate
ACO	1-aminocyclopropane-1-carboxylate oxidase
ACS	1-aminocyclopropane-1-carboxylic acid synthase
AOC	allene oxide cyclase
AOS	allene oxide synthase
cDNA	complementary deoxyribonucleic acid
DAMPs	damage-associated molecular patterns
dpi	days post inoculation
dpw	days post wounding
ET	ethylene
GLM	generalized linear model
GLMM	generalized linear mixed model
HAMPs	herbivore-associated molecular patterns
JA	jasmonic acid
JA-Ile	jasmonic acid-isoleucine
JAZ	jasmonate ZIM-domain
LOX	lipoxygenase
MPB	mountain pine beetle
OPDA	cis-(+)-12-oxophytodienoic acid
OPR3	12-oxo-phytodienoic acid reductase
PAMPs	pathogen-associated molecular patterns

PRRs	pattern recognition receptors
PTI	pattern-triggered immunity
qRT-PCR	quantitative reverse transcription polymerase chain reaction
SA	salicylic acid
UBA1	Ubiquitin-activating enzyme
UBC11	Ubiquitin-conjugating enzyme 11
VHA-A	Vacuolar ATP synthase subunit A

Chapter 1: Introduction

1.1 Lodgepole pine

The lodgepole pine (*Pinus contorta* Dougl.) is a coniferous species with mature specimens reaching heights of up to 30 m and diameters of approximately 60 cm. It has needle-like leaves, arranged in pairs within bundles, measuring 3 to 7 cm in length. The cones of the lodgepole pine are 3-6 cm long and feature a curved prickle at the tip of each scale. The bark is thin and varies in color from orange, brown to grey, with fine scales (Natural Resource Canada, Canadian Forest Service 2015).

Lodgepole pine is a major component of forest ecosystems in western North America , with a wide distribution that extends from British Columbia southward to the United States along the Rocky Mountains and eastward to Alberta (Carlson et al. 2000). In western Canada, lodgepole pine forests comprise roughly 35% of the forested areas in the provinces of British Columbia and Alberta (Critchfield 1985).

In Canada, there are two subspecies or varieties of lodgepole pine: *Pinus contorta* Dougl. ex. Loud. var. *latifolia*, commonly known as lodgepole pine, and *Pinus contorta* Dougl. ex. Loud. var. *contorta*, also called shore pine, which is shorter and shrubbier than the lodgepole pine and is limited to the coastal regions of British Columbia (Figure 1.1) (Richardson 2000). This study focuses on *Pinus contorta* Dougl. ex. Loud. var. *latifolia*, the only lodgepole pine variety found within the province of Alberta. It is characterized as an early successional and fire-adapted

Cordilleran species. It thrives in areas with less fertile and coarser-textured upland soils, as well as along the margins of bogs. Furthermore, *Pinus contorta* Dougl. ex. Loud. var. latifolia exhibits notable adaptability to the unique environmental conditions found in the mountains and foothills of Alberta (Rweyongeza 2010).

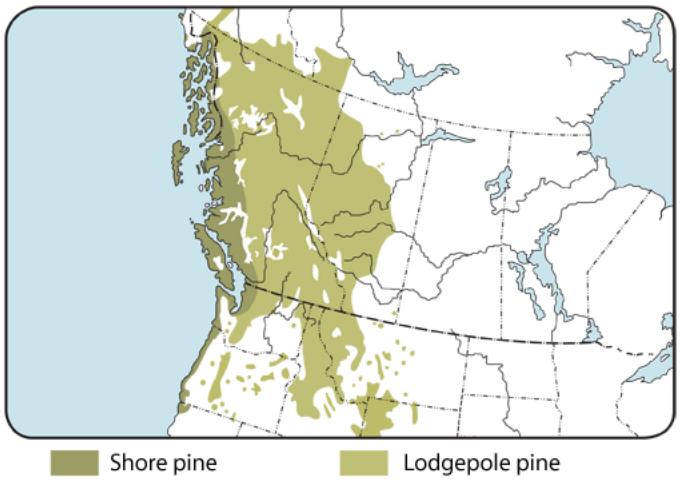

Figure 1.1: Approximate species ranges in Canada for shore pine (*Pinus contorta* Dougl. ex. Loud. *var. contorta*) shown in dark green and lodgepole pine (*Pinus contorta* Dougl. ex. Loud. *var. latifolia*) shown in light green. Distribution map was obtained from Natural Resource Canada, Canadian Forest service (https://tidcf.nrcan.gc.ca/en/trees/factsheet/140, accessed October 09, 2023).

1.2 Mountain pine beetle

Lodgepole pine is frequently subjected to attacks by insect herbivores. Native to western North America, mountain pine beetle (MPB, *Dendroctonus ponderosae* Hopkins) is a bark beetle which overcomes host defenses through a mass attack strategy (Cullingham et al. 2011).

The life cycle of bark beetles comprises three fundamental phases (Figure 1.2). Following successful mass attack, adult beetles colonize a host tree, simultaneously navigating the tree's chemical defenses. During this phase, they construct vertical galleries in the tree's phloem and engage in mating, depositing eggs within these galleries. The second phase involves hatching and overwintering, the larvae develop beneath the tree's bark and establish feeding galleries perpendicular to the parental galleryan. A key element influencing the growth of MPB populations is the mortality rate of larvae during winter, the hatched larvae overwinter under the bark of a tree host, producing cryoprotectants like glycerol to survive the cold temperature (Bentz *et al.* 1999; Bale *et al.* 2002). The final phase entails emergence from the host tree and dispersal to seek new hosts. Young adult beetles sustain themselves by consuming microorganisms, such as MPB fungal associates, within the galleries before emerging during the summer, marking the commencement of a cyclical annual life cycle (Raffa et al. 2015; Khadempour et al. 2012). MPB spends most of its life cycle residing within its host organism, with the notable exception of its dispersal phase. This phase predominantly takes place when the adult beetles emerge from their host, which typically happens from July to August (Safranyik and Carroll 2006). In general, the reproductive cycle of MPB is characterized as univoltine, implying that it typically gives rise to only one generation each year. However, divoltine cycles have been observed. In these cycles, when environmental conditions are particularly conducive, the MPB can produce two generations within a single year (Safranyik and Carroll 2006).

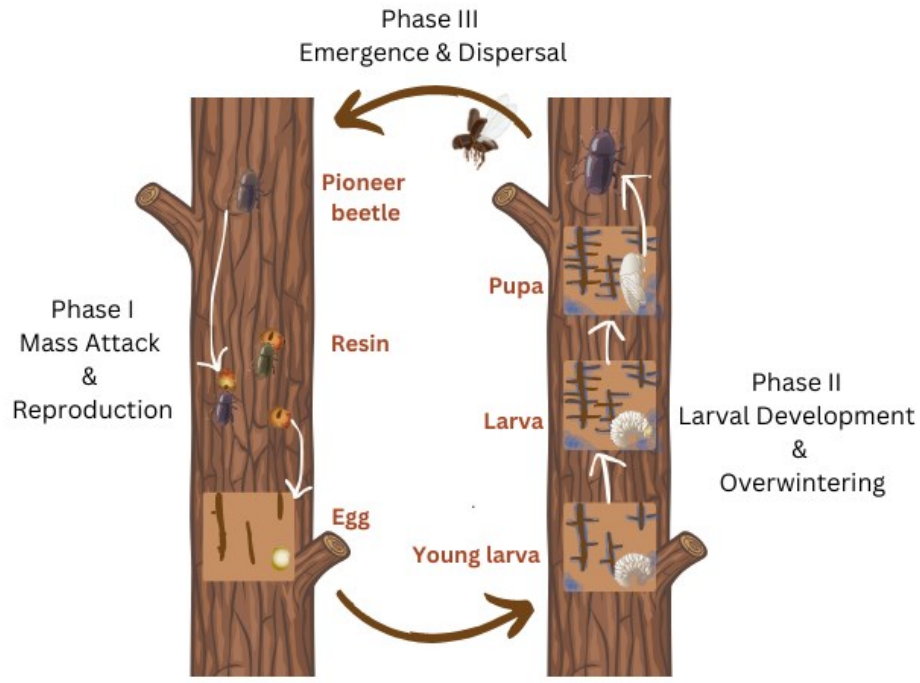

Figure 1.2: Life Cycle of the Mountain Pine Beetle (MPB, *Dendroctonus ponderosae* Hopkins). This figure delineates the three critical phases in the MPB's annual cycle: Phase I, mass attack and reproduction, where beetles overcome tree defenses and establish vertical galleries for mating and egg deposition; Phase II, larval development and overwintering, with larvae establishing feeding galleries beneath the tree's bark perpendicular to parental galleries; Phase III, the emergence of young adult beetles, who feed on microorganisms within the galleries before dispersing in summer to seek new hosts.

MPB is an eruptive forest insect, with its populations fluctuating between low-density endemic phases and high-density epidemic (outbreak) phases (Raffa et al. 2008). When MPB populations are in the endemic state, damaged trees or trees with compromised defence capacity are MPB's primary target of infestation. If the conditions are right, MPB populations erupt into large-scale

outbreaks. MPB employs a mass attack strategy, to effectively establish itself in a host tree. The strategy is initiated when the first bark beetle targets a tree and secretes an aggregation pheromone. This chemical cue serves to attract other bark beetles from nearby areas. Subsequently, the arriving beetles also emit additional pheromones to strengthen the collective signal and increase the probability of a successful collective attack on the tree (Wood 1982). Because of the mass attack strategy, MPB then can overcome the host defenses of larger healthy pines, which serve as a better source of nutrition for larvae arise from the eggs produced by attacking female beetles. The ability of MPB to attack large healthy trees in the epidemic state of an outbreak results in significant losses of mature healthy strands (Safranyik & Carroll 2006).

MPB has significantly impacted on Canada's forests, with its distribution and effects evolving over time. This outbreak has primarily targeted the lodgepole pine, a species with which the MPB shares a long evolutionary history and which constitutes one of its main hosts (Cullingham et al. 2011; Erbilgin et al. 2014). The lodgepole pine's range notably overlaps with the MPB's historic range, which was predominantly confined to British Columbia (Safranyik et al. 2010). This alignment between the beetle's preferences and its traditional habitat has historically localized the majority of MPB outbreaks to this region (Cudmore et al. 2010).

Since the early 1990s, the outbreak has resulted in the devastating loss of over 18 million hectares of forest within British Columbia, marking a significant environmental and ecological impact (Corbett et al. 2016; Dhar et al. 2016). This situation demonstrates the extent to which the lodgepole pine, and consequently the forests of British Columbia, are vulnerable to MPB infestations.

However, the outbreak's dynamics began to shift in 2006 when the MPB expanded its range into northern Alberta (Cullingham et al. 2011; Bentz et al. 2010). This marked a significant development as it showed the beetle populations' capability to successfully infest a novel host, the jack pine (Pinus banksiana Lamb.), in Alberta (Dhar et al. 2016), This adaptation to a new host species indicates the beetle's potential to threaten a broader range of forest ecosystems beyond its historic confines.

Following this expansion into Alberta, the MPB outbreak has continued to spread, moving northward into the Northwest Territories and eastward through Alberta towards Saskatchewan (James & Huber 2019). This progression highlights a concerning trend of geographic and host expansion that could pose a threat to the vast boreal forest that spans across Canada (Safranyik et al. 2010; Burns et al. 2019).

The current trajectory of the MPB outbreak, with its ability to adapt to new environments and hosts, suggests a looming threat of further eastward spread (Brush & Lewis 2023). This potential for a wider infestation across Canada's boreal forests underscores the urgency for monitoring and managing the MPB outbreak to mitigate its impact on these critical ecosystems.

1.3 Components of conifer defense response

1.3.1 Constitutive defenses in conifers

To defend against attack, lodgepole pine have evolved both constitutive and inducible defense mechanisms (Franceschi et al. 2005). Constitutive defenses are pre-formed protections that are consistently present in trees, serving as a barrier against a broad spectrum of organisms attempting to infiltrate the bark. These constitutive defenses encompass multiple layers of both mechanical and chemical defenses (Franceschi et al. 2005). Mechanical defenses, such as suberized and lignified cell layers, sclereid stone cells, and calcium oxalate crystals in conifers, provide physical toughness to the bark, making it difficult for herbivores to penetrate (Hudgins et al. 2003; Whitehill et al. 2019). Trees possess a complex bark structure comprising over 10 distinct cell types, including phloem sieve cells specialized in sugar transport (Celedon et al. 2017). This diversity not only supports various tree functions but also makes the phloem a target for stem-feeding insects like bark beetles, drawn to its nutrient-rich content (Soderberg et.al. 2021). In response to the threat posed by these beetles, which can severely impact tree survival by damaging the vascular tissue, trees have developed a multi-layered defense system. The outermost layer, the periderm, acts as a physical barrier. Beneath it, the cortex layer contains toxic phenolic compounds, deterring invaders. Finally, the secondary phloem tissue, located below the cortex, originates from the cambium meristem and incorporates additional defenses, both mechanical and chemical, to protect the tree (Franceschi et al. 2005).

Constitutive chemical defenses involve the storage and subsequent release of various compounds when under attack. These compounds encompass phenolics, terpenoids, alkaloids, toxins, defensive proteins, enzymes, and resins. These defenses are dispersed throughout the various tissues, which include the periderm, cortex, secondary phloem and secondary xylem (Franceschi et al. 2005). In pines, both xylem and phloem tissues contain resin-producing structures, essential for the tree's defense, particularly against bark beetles and associated fungi (Hudgins et al. 2004; Fett-Neto & Rodrigues-Corrêa 2012). The resin, a terpenoid mixture primarily composed of monoterpene and sesquiterpene-rich turpentine and diterpenoid-rich rosin, plays a crucial role in this defense mechanism (Rodrigues-Corrêa et al. 2012). It is continuously produced, stored, and maintained under pressure within specialized resin ducts. This pressurization facilitates its rapid release in response to pest attacks, exposing the invaders to the resin's toxic compounds and effectively repelling them (Huber et al. 2004).

1.3.2 Inducible defenses in conifers

Inducible defenses refer to defense strategies that are synthesized or become active in response to an invasion. These mechanisms boost the overall defensive capabilities of the plant by restricting the extent of damage and sealing injured tissues (Franceschi et al. 2005).

Inducible chemical defenses include phenolics, terpenoids and defense proteins that are induced by pines in response to pathogen and insect challenge. Phenolics are abundant in conifer bark, and serve as antifungal agents and antifeedants (Franceschi et al. 2005). When bark is invaded, there's a swift increase in the production of phenolics or the upregulation of enzymes, with the phenolics

induced by such invasions being more toxic or specifically targeted against the invaders than those that are always present (Franceschi et al. 2005; Richard et al. 2000). An anatomical feature in Pinaceae, the polyphenolic parenchyma (PP) cells located in the phloem, plays a crucial role in storing and synthesizing these phenolic compounds (Li et al. 2012; Nagy et al. 2014). These cells respond to damage or pathogen attack by swelling and increasing their phenolic content, ready to release these compounds if broken by insects or fungal growth (Franceschi et al. 1998, 2005). Moreover, phenolics can also accumulate in the xylem around infection sites, forming reaction zones and lesions (Nagy et al. 2012, 2022). The oxidation of these accumulated phenolics leads to wood discoloration, a visual indicator of the tree's defensive response (Liu et al. 2021). Lesions rich in phenolics develop in response to both natural attack by MPB and its fungal symbionts *G. clavigera*, and inoculation with *G. clavigera* (Arango-Velez et al. 2014; Arango-Velez et al. 2016).

In conifer species, a crucial defense mechanism against injury or attack is the development of traumatic resin ducts. These ducts, which can be axial, radial, or form resin blisters, are found throughout the phloem, xylem, and needles (Chiu and Bohlmann 2022; Celedon and Bohlmann 2019; Vázquez-González et al. 2020). When a tree is wounded or attacked, these ducts form both above and below the site of injury, enabling the transport of toxic terpenoid compounds to repel the invasion (Nagy et al. 2000). Observations from North American pine species reveal a direct correlation between survival rates after bark beetle attacks and the presence of more or larger resin ducts, suggesting that trees with enhanced resin duct production are better equipped to withstand such threats (Kane and Kolb, 2010; Ferrenberg et al., 2014; Gaylord et al., 2015; Hood et al., 2015; Zhao and Erbilgin, 2019). Furthermore, the activation of existing resin ducts significantly increases oleoresin production in response to wounding, pathogen challenges, or insect attacks, effectively

creating a barrier against further damage (Vázquez-González et al. 2020; Keeling & Bohlmann 2006; Eyles et al. 2010).

Increased production of resin ducts in conifers enhances resistance to pests by boosting terpene synthesis, which are key chemical defenses (Raffa, 2014). Terpenes, ubiquitous across plant species, vary within individuals of the same species, across geographic locations, and in response to stress, underscoring their adaptability and defensive utility (Keeling and Bohlmann 2006; Pureswaran et al. 2004; Kopaczyk et al. 2020). These compounds not only serve as structural defenses within oleoresin but are also toxic to certain insects, such as MPB, at specific concentrations, highlighting their role in pest deterrence (Chiu et al. 2017). The diversity in terpenoid composition produced by trees may influence the attractiveness of hosts to pests like MPB, suggesting a complex interaction between plant chemistry and pest behavior (Raffa et al. 2013).

Another type of induced defenses in plants is the hypersensitive response, which occurs at the infection site and involves the production of reactive oxygen species and rapid cell death. This response is aimed at killing and containing various pathogens like fungi, bacteria, and viruses (Bleiker & Uzunovic 2004; Franceschi et al. 2005). A more general response to damage is the formation of wound periderm. Callus tissue can be lignified, suberized, or impregnated with phenolics, and form part of wound periderm. This tissue acts as a defense mechanism, preventing further intrusion and isolating fungal pathogens (Franceschi et al. 2005). Peroxidases play a crucial role in neutralizing harmful reactive oxygen species that can accumulate during tissue damage or as part of the plant's hypersensitive response to pathogen attack (Pan et al. 2018). These enzymes

are categorized as Pathogenesis-related (PR) proteins, which also encompass chitinases, thaumatin-like proteins (also known as osmotins), and defensins (Van Loon et al. 2006). PR proteins are not typically found in healthy tissues but are quickly produced in both the affected area and throughout the plant in reaction to pathogen exposure (Van Loon et al. 2006). Among the PR proteins, chitinases break down chitin, a major component of fungal cell walls, thereby inhibiting fungal growth (Neuhaus 1999). Thaumatin-like proteins, with their anti-fungal properties, play a key role in the plant's defense by directly targeting fungi (Liu et al. 2010). Their mechanism involves disrupting the structure of fungal cell walls, effectively halting the development of fungal hyphae and thereby limiting fungal proliferation (Abad 1996; Osmond 2001). Defensins, which are small antimicrobial peptides, are found throughout almost all plant tissues and are a fundamental component of the plant's innate immune system (Lacerda et al. 2014).

1.3.3 Pathogen recognition and activation of defense response

Host plants have developed sophisticated strategies to detect and defend against various invaders, enabling them to respond more effectively to threats. One of the key mechanisms in this defensive strategy involves Pattern Recognition Receptors (PRRs), which are specialized receptors located on the surface of plant cells, they play a crucial role in identifying small molecules emanating from antagonistic agents (Zipfel 2014). These PRRs are capable of binding to and recognizing distinct molecular patterns that are typically associated with foreign invaders. This process is a vital part of the plant's initial detection and response system against pathogens, whether they are necrotrophic or biotrophic, plants specifically identify pathogen-associated molecular patterns (PAMPs), which are unique molecular signatures characteristic of these

invaders (Glazebrook 2005). Additionally, plants have evolved to detect herbivore-associated molecular patterns (HAMPs) like insect oral secretions and damage-associated molecular patterns (DAMPs) from the host itself, released during wounding or digestion by pathogens or herbivores (Choi and Klessig 2016). After recognizing an antagonist through PRRs, a host plant can initiate a broad defense response known as pattern-triggered immunity (PTI) (Zipfel 2014). However, pathogens have developed the ability to adjust to the genotypes of their hosts and secrete virulence factors known as effectors, which can undermine the basic defenses of the host by suppressing the PTI mechanisms. (Karasov et al. 2014; Raffaele et al. 2010; Dangl et al. 2013; Deslandes et al. 2012). In response to this, plants have evolved a mechanism to detect these effector molecules through a set of diverse intracellular receptors known as nucleotide-binding/leucine-rich-repeat (NB-LRR) receptors. Activation of these receptors triggers effector-triggered immunity (ETI), which is an enhanced and more intense form of defense than PTI (Cui et al. 2015).

There's a prevailing theory suggesting that ETI essentially represents a more rapid and intensified version of PTI (Jones & Dangl 2006). Recent studies indicate that PTI serves as the initial defense line against pathogen invasion. Pathogens, in turn, deploy effectors to neutralize PTI, marking a critical pathogenic strategy. NLR signaling enhances certain aspects of PTI signaling, serving as compensation for the suppression of PTI by pathogens or the plant's own negative regulatory mechanisms (Yuan et al. 2021; Ngou et al. 2021). ETI, therefore, is not an independent immune response but rather acts as an augmentation of the PTI system, relying on the foundational PTI components to be effective (Yuan et al. 2021).

1.3.4 Plant hormones involved in regulating induced defense response

Plant hormones like jasmonic acid (JA), ethylene (ET) and salicylic acid (SA) play important roles in regulating the induced defense responses (Pieterse et al. 2009, Bürger & Chory 2019). During induced defense responses, the plant hormones are part of a signaling network that activates a plant's defense response. SA is involved in response to biotrophic pathogens, and JA is crucial for activating plant's responses against wounding, necrotrophic pathogens, and herbivorous insects such as MPB (Arango-Velez et al. 2016; Bürger & Chory 2019). Moreover, in plant defense against necrotrophic pathogens, ET is also a crucial signaling molecule acting independently or synergistically with JA in regulation of these responses (Bürger & Chory 2019). There is also evidence in angiosperms for antagonistic crosstalk between JA and ET in responses to herbivores, where ET can act to inhibit JA-mediated signalling (Erb & Reymond 2019). ET signalling has also been implicated in defense and repair pathways that are activated upon wounding (Heyman et al. 2018).

The JA pathway is recognized as a key signal transducer that induces various plant secondary metabolites (Zhao et al. 2004). JA is synthesized from alpha-linolenic acid (C18:3), a fatty acid obtained from chloroplast membranes (Figure 1.2). This synthesis occurs through a series of sequential reactions facilitated by specific enzymes in chloroplasts, the first step is to synthesize (13S)-hydroperoxyoctadecatrienoic acid under the action of lipoxygenase (LOX), next two-step reaction of membrane-associated allene oxide synthase (AOS) is occurred, whose highly unstable product is cyclized by an allene oxide cyclase (AOC) to cis-(+)-12-oxophytodienoic acid (OPDA),

and it reduced by 12-oxo-phytodienoic acid reductase (OPR3) in peroxisomes followed by β-oxidation to form JA (Figure 1.2) (Wasternack & Song 2017, Bürger & Chory 2019).

Once JA is produced, it quickly combines with the amino acid isoleucine (Ile) to form bioactive JA-Ile, due to the action of jasmonate-amino acid synthetase. To mediate JA responses, SCF^{COI1} E3 ligase directly binds to JA-Ile. The jasmonate ZIM-domain (JAZ) proteins function as substrates of the SCF^{COI1} complex and engage in interactions with the transcription factor MYC2 to inhibit the jasmonic acid (JA) signaling pathway. Upon receiving a JA signal, the COI1 protein interacts with the JAZ proteins and facilitates their ubiquitination, leading to their subsequent degradation via the 26S proteasome. This degradation process releases downstream transcription factors, enabling them to regulate gene expression and initiate JA-responsive pathways (Figure 1.2) (Wasternack & Song 2017).

JA, including its derivative methyl jasmonate (MJ) has been implicated in stimulating induced conifer defenses, such as upregulating terpene biosynthesis (Franceschi et al. 2002, Martin et al. 2002, Zeneli et al. 2006, Vazquez-González et al. 2022). Application of MJ can induce formation of traumatic resin ducts, where terpene-containing resin is synthesized and transported (Franceschi et al. 2002, Martin et al. 2002). Arango-Velez et al. (2016) demonstrated that both JA and JA-Ile are synthesized by lodgepole pine seedlings in response to *G. clavigera* challenge. Similarly, in the context of other conifer species, such as the Norway spruce, research by Arnerup et al. (2013) has highlighted the critical role of JA-mediated signaling as a key defense mechanism against necrotrophic fungal pathogens. More recently, Fortier et al. (2024) showed that *G. clavigera*-inoculated mature lodgepole pine trees also synthesize JA and JA-Ile. These studies demonstrating

host production of JA and JA-Ile in response to *G. clavigera* challenge provided a line of evidence that *G. clavigera* is acting as a necrotrophic rather than a biotrophic pathogen, and perception by lodgepole pine activates the JA signalling pathway. Importantly, Fortier et al. (2024) showed significant increases in JA and JA-Ile *in planta* levels in response to MPB attack of lodgepole pine, providing direct evidence of JA and JA-Ile involvement in pine defense against herbivorous bark beetles.

Previously, there was no research on ethylene-associated gene expression in response to pathogen attack. However, Fortier et al. (2024) demonstrated that *G. clavigera* inoculation of mature lodgepole pine induces synthesis of the ET precursor, 1-aminocyclopropane-1-carboxylate (ACC). ACC is often used as a measure of ET biosynthesis because ET is a gaseous compound, and therefore much more challenging to accurately measure than its precursor ACC (Bulens et al. 2011). ACC is synthesized by 1-aminocyclopropane-1-carboxylic acid synthase (ACS), and it is catalyzed into ET by 1-aminocyclopropane-1-carboxylate oxidases (ACO) (Figure 1.2; Dong et al. 1998). ET perception occurs through the binding of ET to multiple receptors. In *Arabidopsis thaliana*, these are ethylene response 1 (ETR1), ethylene response 2 (ETR2), ethylene insensitive 4 (EIN4), ethylene response sensor 1 (ERS1), and ethylene response sensor 2 (ERS2). These receptors play a role as negative regulators, suppressing ET signaling. In the absence of an ET signal, the ET receptors activate a Raf-like kinase called constitutive triple response 1 (CTR1), which in turn exerts negative regulation on the downstream ET response pathway by inactivating ethylene insensitive 2 (EIN2). However, upon binding of ET, the receptors are inactivated, leading to the deactivation of CTR1. Consequently, EIN2 assumes a positive regulatory role in the ET signalling pathway. The ethylene (ET) signal is transmitted through the intermediary molecule

EIN2 from ET receptors located on the endoplasmic reticulum (ER) to nuclear-localized transcription factors ethylene insensitive 3 (EIN3) (Zhu and Guo, 2008; Ji and Guo, 2013). EIN3 binds to the promoter region of the ethylene response factor (ERF1) gene and activates its transcription, thereby initiating downstream ET responses (Figure 1.2; Azoulay et al. 2023).

While ET signalling is canonically associated with plant responses to necrotrophic pathogens in angiosperms (Bürger & Chory 2019), wounding – including both mechanical wounding and wounding caused by herbivores and pathogens – has also been demonstrated to involve ET (Heyman et al. 2018). ET may also be involved in mediating repair of wounded tissues (Heyman et al. 2018). Application of ET to conifers such as Douglas-fir (*Pseudotsuga mensziesii*) and sequoia (*Sequoiadendron giganteum*) can induce development of traumatic resin ducts (Hudgins and Franceschi 2004), important in defense of conifers against both pests and pathogens.

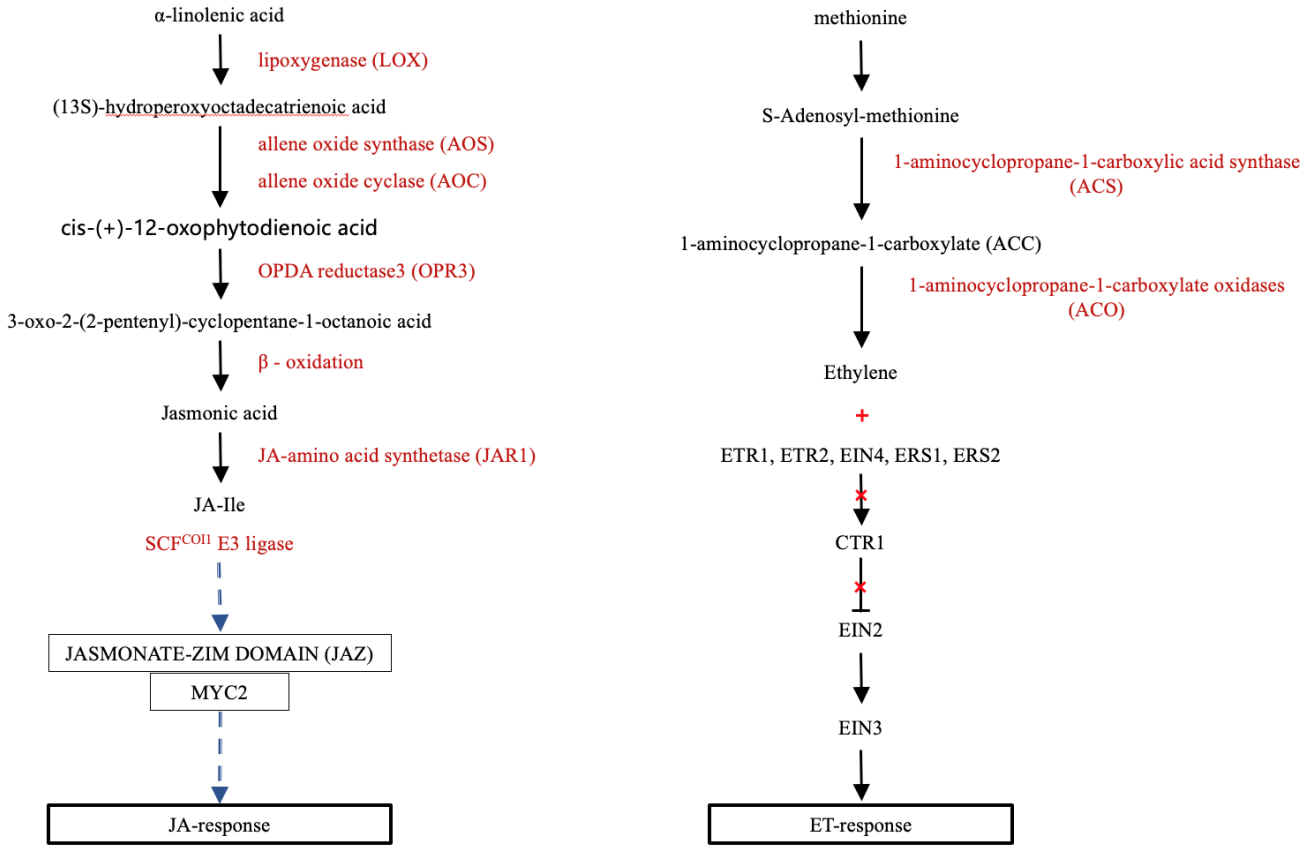

Figure 1.3: Biosynthesis and signaling pathways of JA and ET. These pathways reflect our current understanding of JA and ET biosynthesis and signalling in *Arabidopsis thaliana* (modified from: Wasternack & Song 2016; Li et al. 2019; Zhu 2014). Synthesis of JA/JA-Ile occurs from alpha-linolenic acid, involving the known enzymes: lipoxygenase (LOX); allene oxide synthase (AOS); allene oxide cyclase (AOC); OPDA reductase3 (OPR3);JA-amino acid synthetase (JAR1). JA-Ile perception and signaling occur via the SCFCOI1–JAZ co-receptor complex. The JAZ repressors interact with the transcription activator MYC2 and activate the JA-response. The synthesis of ET from methionine involves the enzymes: 1-aminocyclopropane-1-carboxylic acid synthase (ACS); 1-aminocyclopropane-1-carboxylate oxidases (ACO). ET binds to five receptors:

ethylene response 1 (ETR1), ethylene response 2 (ETR2), ethylene insensitive 4 (EIN4), ethylene response sensor 1 (ERS1), and ethylene response sensor 2 (ERS2), leading to the deactivation of constitutive triple response 1 (CTR1). The removal of the inactivation of ethylene insensitive 2 (EIN2) activates ethylene insensitive 3 (EIN3), initiating the ET response.

1.4 Roles of MPB ophiostomatoid fungal symbionts in MPB-host tree interactions

MPB form symbioses with ophiostomatoid (blue-stain) fungal species. One of the most prevalent MPB fungal symbionts is the pathogenic fungal species called *Grosmannia clavigera* [Robinson-Jeffrey and Davidson] Zipfel, de Beer and Wingfield, *Ophiostoma montium* (Rumbold) von Arx., and *Leptographium longiclavatum* Lee, Kim and Breuil (Bleiker et al. 2009; Roe et al. 2011; Six 2020). It belongs to the ophiostomatoid blue stain fungal species and acts as a necrotrophic pathogen (Raffa & Berryman 1983). Necrotrophic pathogens are known for killing host tissues to extract nutrients from cells that are dead or in the process of dying (Glazebrook 2005). In contrast, another category of pathogens, known as biotrophs, obtains nutrients from living tissues (Glazebrook 2005). However, many pathogens exhibit dual behavior, acting as necrotrophs under certain conditions or during specific life cycle stages, while functioning as biotrophs in other scenarios. These adaptable pathogens are termed hemi-biotrophs (Glazebrook 2005).

G. clavigera induces chemical and anatomical changes during inoculation with trees (Lusebrink et al. 2013; Arango-Velez et al. 2014), similar to those observed in beetle-attacked trees (Raffa & Smalley 1995; Franceschi et al. 2005). Following successful attack of a host pine tree, the beetles mine lateral galleries in the bark while *G. clavigera* invades the phloem and sapwood (Paine et al.

1997; Solheim & Krokene 1998; Six et al. 2003). As they enter the adjacent phloem and sapwood host tissues, these fungi produce the polyketide pigment melanin, which causes a blue or gray discoloration of the wood of the host tree (Lee et al. 2006). Pine trees have developed complex defense mechanisms to combat pests and pathogens, prominently featuring the formation of lesions rich in secondary metabolites (Franceschi et al. 2005, Witzell and Martín 2008). As described in Section 1.3.2, a key aspect of this defense involves PP cells located in the phloem, which are crucial for storing and synthesizing phenolic compounds (Li et al 2012, Nagy et al 2014). When pine trees are attacked by pathogens such as MPB and its fungal symbionts, the PP cells can swell and multiply in response to attacks, releasing phenolic compounds into the xylem, where they form reaction zones and lesions (Franceschi et al 1998, 2005; Nagy et al 2012, 2022). The oxidation of these phenolics leads to the discoloration of wood, producing darkened lesions (Liu et al 2021). These lesions, extending vertically and radially from the infection site within the sapwood. This lesion is composed of cells which contain large quantities of defensive chemicals (Francheschi et al 2005).

The relationship between MPB and *G. clavigera* is mutualistic, both have evolved traits that benefit each other. These fungal symbionts play a critical role in the MPB's successful colonization by compromising the pine host's defenses (Lieutier et al. 2009). In addition, *G. clavigera* possess the ability to neutralize some of the defense compounds produced by the host trees, as described in Section 1.3 (DiGuistini et al. 2011). On the other hand, there is a deep interdependence between MPB and its fungal associate. The reproduction of MPB is heavily reliant on the presence of these fungal associates (Six and Paine 1998), similarly, these fungi depend on the MPB for their spread (Bleiker et al. 2009, Six 2020).

Neither the individual effects of beetle damage to the phloem nor fungal inoculation alone result in the rapid tree mortality required for beetle colonization, but it is the combined influence of both factors that is essential for the survival and reproduction of the beetles (Klutsch et al. 2017). Due to the complex relationship between MPB and fungal associates, the practice of inoculating with *G. clavigera* is often employed as a stand-in for studying the effects of MPB attacks (McAllister et al. 2018).

There is considerable evidence that these fungi provide nutrition for the beetle and developing larvae (Safranyik & Carroll 2006; Six & Paine 1998). The fungi achieve this by colonizing the tree's ray cells and xylem, where they translocate nutrients to the beetle's feeding and breeding areas (Six 2020). This not only supports the fungi's own growth and reproduction but also enriches the beetle's diet with increased nitrogen, sterols, and other vital nutrients. (Klepzig and Six 2004; Bentz and Six 2006; Cook et al. 2010, Goodsman et al. 2012; Six and Klepzig 2021). After maturing, new MPB adults spend a short period under the bark feeding on the fungi lining their pupal chambers. During this time, they collect fungal spores on their exoskeleton and in specialized structures known as mycangia (Safranyik & Carroll 2006). These spores, which are produced by the fungi on specialized fruiting bodies designed for beetle dispersal, are sticky and well-adapted for transport to new host trees (Six & Klepzig 2004).

There has been a long-standing question of whether ophiostomatoid fungal associates of MPB such as *G. clavigera* contribute to the beetle's capacity to overcome defenses of healthy trees during the attack phase (Bleiker and Six 2007, Goodsman et al. 2012), or whether the primary role

of these ophiostomatoid fungi is to contribute to MPB's nutrient budget as described above (Table 1.1, Six and Wingfield 2011).

The paradigm that ophiostomatoid fungal symbionts contribute to MPB's ability to overwhelm host defenses has been primarily based on the observation that these ophiostomatoid species cause harm to the host and elicit canonical defense responses following their introduction to the host tree by MPB (Leutier et al. 2009). This is also evidenced by the fact that trees inoculated with *G. clavigera* display similar defense mechanisms to those observed during MPB attacks (Arango-Velez et al. 2014, 2016). The prevailing is challenged by evidence showing that such beetles can cause tree death independently of these pathogens. This is exemplified by *Dendroctonus ponderosae*, the most significant pine pest in North America, which does not need its virulent fungal associates to induce tree mortality (Six & Bentz 2007). Conversely, there are bark beetles that do not result in tree death but are associated with highly virulent fungal partners. Examples include lodgepole pine beetle, black turpentine beetle and red turpentine beetle, which can all develop within living trees without killing them (Spatafora et al. 1994). Despite not being lethal to their hosts, these beetles are often found in association with *Leptographium terebrantis*, one of the most virulent fungi among the Ophiostomatales associated with bark beetles (Six & Wingfield 2011). This suggests a complex relationship between bark beetles and their fungal associates that does not strictly correlate with the beetles' ability to kill trees.

In the latter case, Six and Wingfield (2011) provide evidence in their review that these fungi offer an advantage in competing with other species of the MPB microbiome, allowing these fungi to colonize the host for resource capture more effectively instead of contributing significantly to bark

beetles' ability to overcome the trees' induced and constitutive defenses. Bleiker & Six (2007) demonstrated that *G. clavigera* transports nitrogen and phosphorus from deep within the tree to the phloem, where beetle larvae and newly emerged adults feed. This process makes essential nutrients accessible to the developing larvae, indicating that the reproduction of MPB is significantly dependent on these fungal associates, as highlighted by Six and Paine (1998).

In their recent study, Fortier et al. (2024) demonstrated that natural attack of lodgepole pines by MPB induces significant JA biosynthesis by the host during the mass attack phase but does not induce ET biosynthesis. They employed liquid chromatography-tandem mass spectrometry (LC-MS/MS) to measure the levels of the ET precursor ACC, along with JA and its active form, JA-Ile, in lodgepole pines subjected to mass attacks by MPB and those inoculated with the fungal pathogen *G. clavigera*. JA is known to be essential for activating plant defenses against wounding, necrotrophic pathogens, and herbivorous insects such as the MPB. ET is also a crucial signaling molecule acting independently or synergistically with JA to regulate responses to necrotrophic pathogens. To investigate if the combined JA and ET response, typically triggered by necrotrophic fungal pathogens, is also present in lodgepole pines attacked by MPB, the study examined whether *G. clavigera* inoculation would induce the biosynthesis of both JA and ET. The findings revealed that levels of JA, JA-Ile, and the ET precursor ACC all increased following *G. clavigera* inoculation, indicating a defense response similar to that against necrotrophic fungal pathogens. However, in trees attacked by MPB, while JA and JA-Ile levels did increase, consistent with a response to herbivorous insect pest attack, ACC levels did not show an increase (Table 1.1).

Table 1.1: Testing the classic paradigm using hormones. This table examines the hypothesis that ophiostomatoid fungi contribute to the mountain pine beetle's (MPB) ability to overwhelm host defenses during the mass attack phase. If ophiostomatoid fungi are influential, lodgepole pine should perceive an attack by both MPB and necrotrophic pathogen, triggering the synthesis of both jasmonic acid (JA) and ethylene (ET). Alternatively, if these fungi do not meaningfully enhance MPB's attack capacity, the pine should perceive only the MPB, resulting in increased levels of JA but not ET. The experimental results indicate that *G. clavigera* does not significantly contribute to MPB's ability to overcome lodgepole pine defenses, as evidenced by the observed increase in JA levels without a corresponding increase in ET levels after MPB attack.

Contribution of *G. clavigera* to mass attack	Response to *G. clavigera* and mass attack	Hormone production
YES	similar	JA & ET ↑
NO	different	JA & ET ↑ for *G. clavigera* JA ↑ for MPB

These data provide the first experimental evidence that the host tree is responding only to the herbivorous insect during the attack phase, and not to the necrotrophic ophiostomatoid fungal associates such as *G. clavigera* that are vectored by MPB. These results suggest that ophiostomatoid fungi that are introduced into the host by naturally attacking MPB do not

contribute to the capacity of MPB to overcome host defenses during mass attack. Rather, the results suggest that *G. clavigera* and other ophiostomatoid fungal symbionts of MPB begin to colonize plant tissues as the mass attack phase of MPB – host pine interactions give way to the colonization phase. This scenario supports the model that ophiostomatoid fungal associates of MPB contribute to the success of MPB via resource capture.

1.5 Current Study

Building upon the recent study of Fortier et al. (2024) comparing hormone profiles of MPB-attacked versus *G. clavigera*-inoculated mature lodgepole pine during the mass-attack phase of MPB-host interactions described in the previous section, the question that we want to research is: will gene expression patterns for JA and ET biosynthesis and signalling genes reflect the same pattern as the hormone steady state levels that were measured in this experiment? Are JA biosynthesis and signaling genes, but not ET biosynthesis and signaling genes, significantly upregulated in MPB-attacked pines during the mass attack phase? Conversely, are both JA and ET biosynthesis and signaling genes upregulated in *G. clavigera*-infected pines?

My hypothesis is that if *G. clavigera* does not significantly contribute to MPB's ability to overcome tree defenses during mass attack, the tree's response should reflect perception of attack by insect herbivores rather than the necrotrophic fungal phytopathogens that MPB vectors. Because we observed a significant increase in JA levels but not ET levels, I anticipate that only JA biosynthesis and/or signaling genes will be upregulated by lodgepole pine responses to MPB attack during the mass attack phase of host-insect interaction. In contrast, we predict that both ET and JA

biosynthesis and signalling genes will be upregulated in *G. clavigera*-infected pines, consistent with perception of a necrotrophic pathogen by the host.

To test these hypotheses, the objective of my thesis project is to use quantitative reverse transcription polymerase chain reaction (qRT-PCR) transcript abundance profiling to compare expression of JA and ET biosynthesis and signaling genes in lodgepole pine that were attacked by MPB or infected with *G. clavigera*, as described above. The aim is to identify specific genes involved in JA and ET biosynthesis and signaling during MPB and/or *G. clavigera* attack. By gathering additional data on JA and ET biosynthesis and signalling, I intend to further test our theory that *G. clavigera* does not contribute to MPB's ability to overcome lodgepole pine defenses. Because transcript profiles of genes coding for biosynthetic enzymes typically change in advance of changes in levels of their corresponding metabolites, this study of lodgepole pine genes coding for JA and ET biosynthetic enzymes also enabled me to explore potential roles for these hormones in mediating tree responses to MPB during the transition from mass attack to host colonization.

Based on datamining of transcriptome experiments conducted by the Cooke Lab that used microarray (Fortier 2022) and RNA-Seq technologies (Peery et al. 2021) to identify differentially expressed genes in *G. clavigera*-inoculated lodgepole pine, I selected JA biosynthesis genes *PcLOX* and *PcAOS*, the JA transcription factor *PcJAZ*, and the ET biosynthesis genes *PcACO* and *PcACS* for qRT-PCR analysis. I then cloned cDNAs corresponding to these sequences. Since the candidate genes coding for *PcLOX*, *PcAOS*, *PcJAZ*, *PcACO* and *PcACS* all belong to gene families, I carried out *in silico* analyses of the cloned cDNAs to verify that these cDNAs represented the candidate genes chosen for analysis. I then carried out qRT-PCR for each of these genes to

investigate their expression profilines in lodgepole pine responses to natural MPB attack during the mass attack phase versus inoculation with the necrotrophic fungal associate *G. clavigera*.

The results obtained in this project will be used to complement a transcriptome analysis of lodgepole pine responses to MPB attack versus *G. clavigera* inoculation that is being carried out using RNA-Seq.

Chapter 2: Materials and Methods

2.1 Plant Experimental Materials

The same experimental materials used in Fortier et al. (2024) were used for this study. Lodgepole pine trees that were in the prime of their life between 45 to 70 years old were picked which nestled in their natural habitats showing no recent wear or illness. These trees were then split into two groups for our experiments. In the first group, some trees were exposed to *G. clavigera*, with a few kept aside as a control set. The second group involved trees that were left to face an onslaught by MPB naturally, along with their own set of control trees. Timing of the two experiments were staggered to avoid the possibility of *G. clavigera*-inoculated trees being attacked by MPB. Consequently, we conducted the *G. clavigera* experiment right before the MPB started their flight season, whereas the experiment observing MPB attacks took place amidst their active flight period. For the *G. clavigera* inoculation experiment, trees were randomly assigned to one of three groups: 1) *G. clavigera*-inoculated, 2) mock-inoculated, and 3) uninoculated control. Phloem and xylem tissues were collected at 7- and 14-days post-inoculation (dpi) (Figure 2.1). The trees in the MPB-attack experiment were randomly assigned to one of three group: 1) MPB-attacked, 2) mock-attacked, and 3) control (untreated). For this study, we used special lures (Product #3122, from Synergy Semiochemicals Corporation, Delta, BC) tailored for *D. ponderosae* and attached them to the trees targeted in the MPB-attack scenario. This strategy aimed to boost the chances of these trees being chosen by the MPB for attack. We collected samples of both the secondary phloem and secondary xylem at two intervals: 1 day and 7 days following a simulated attack (dpw) (Figure 2.1). Each experimental group had six biological duplicates. Right after collection, we rapidly froze the tissue

samples with liquid nitrogen and kept them on dry ice while they were being transported. For prolonged storage, the samples were moved to a freezer set at -80ºC.

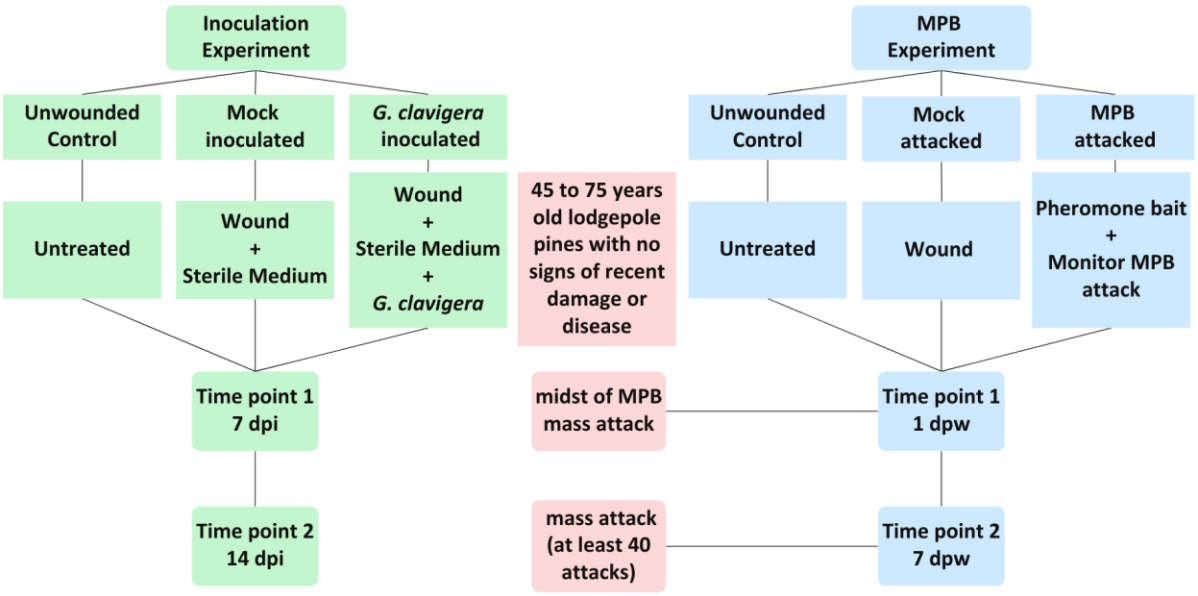

Figure 2.1: Flowchart depicting two experimental setups on mature lodgepole pine trees (Modified from Fortier et al. 2024). On the left, the *G. clavigera* inoculation experiment with treatments assigned to control, mock-inoculated, and *G. clavigera*-inoculated, with samples collected at one- and two-weeks post-inoculation. On the right, the MPB attack experiment is outlined with control, mock-attacked, and MPB-attacked treatments, where tissue samples were gathered between one to three days and one week after the MPB attacks.

2.2 RNA extraction and cDNA Synthesis

The frozen ground tissue between the range of 180 mg to 220 mg was used in the RNA extraction to isolate the intact RNA for gene expression analysis according to the protocol

outlined by Pavy et al. (2008). RNA was extracted by adding a CTAB and β-mercaptoethanol solution to the ground tissue and thoroughly mixing. After incubating the mixture at 65°C and vortexing, chloroform:isoamyl alcohol was added to separate the phases. The aqueous phase was then carefully removed post-centrifugation and the chloroform extraction step was repeated. The volume of the final aqueous phase was measured, a third of the volume of 10M LiCl was added, and the sample was frozen for RNA precipitation. Post-centrifugation, the RNA pellet was washed with ethanol, dried, and then resuspended in nuclease-free water. Agarose gel electrophoresis was used to determine the quality of the RNA, and the concentration of the RNA was quantified with Nanodrop 1000 (Thermo Scientific, ON, Canada). DNase I (NEB) was used to treat RNA, to remove the genomic DNA before DNase inactivation and DNase-treated RNA denaturation. Super Script III (Invitrogen) was used to synthesize cDNA and which was then stored at -20℃ for qRT-PCR analysis.

2.3 Identification of candidate genes

A previously conducted microarray experiment described in Mahon (2016) was mined to identify JA biosynthesis genes *PcLOX* and *PcAOS*, JA signaling gene *PcJAZ* and ET biosynthesis genes *PcACO* and *PcACS* as differentially expressed in lodgepole pine in response to *G. clavigera* inoculation. In this experiment, cDNA of phloem and xylem from *G. clavigera*-inoculated and control (uninoculated, unwounded) lodgepole pine seedlings were hybridized to cDNA microarrays constructed with loblolly pine cDNA probes. Sequences from lodgepole pine transcriptomes were mapped to the heterologous loblolly pine cDNA probes in order to identify genes that were differentially expressed in response to *G. clavigera*. Although this is an older

experiment, mining this dataset provides a starting point for identifying lodgepole pine genes are putatively involved in JA and ET signaling and also differentially expressed in response to G. clavigera. These sequences were then used to identify contigs in a more recently conducted RNA-Seq experiment comparing *G. clavigera* versus control lodgepole pine seedlings (Peery et al. 2021). Subsequently, the obtained sequences were used as queries in a BLASTn search (https://blast.ncbi.nlm.nih.gov/Blast.cgi) against the lodgepole pine master transcriptome (Peery et al. 2021). The open reading frames (ORFs) of target nucleotide sequences were identified and translated to amino acid sequences. In order to identify the function of these genes in other species, a literature search and BLASTx (https://blast.ncbi.nlm.nih.gov/Blast.cgi) were conducted to obtain amino acid sequences from *Arabidopsis thaliana*, *Picea glauca* (white spruce) and *Pinus taeda* (loblolly pine). And then, all amino acid sequences were aligned using the MAFFT (Katoh et al. 2017) plugin for Geneious 2021.1.1 (https://www.geneious.com).The alignments were used to create phylogenetic tree of amino acid sequence in IQ tree (http://www.iqtree.org). The sequence groups most closely related to *A. thaliana* amino acid sequences were selected for primer design.

2.4 Primer design

We aligned all target sequences of *PcLOX, PcAOS*, *PcJAZ*, *PcACO* and *PcACS* matched by BLASTn search against the lodgepole pine master transcriptome using MAFFT (Katoh et al. 2017) and created visualization of the alignment. According to the alignment, the specific regions of target sequences that are most closely related to *A. thaliana* sequence were selected to design primers by Geneious 2021.1.1 (https://www.geneious.com). Cloning primers were

designed to amplify a product size of 1200 base pairs (bp) to 1800 bp, while qRT-PCR primers were designed to amplify a product size of 75 bp to 150 bp. Primer length ranged from 18 bp to 24 bp, melting temperature (Tm) was from 57℃ to 63℃, and GC content was between 20% and 80%. Subsequently, OligoAnalyzer™ Tool (https://www.idtdna.com) was used to analyze the hairpin, self-dimer and hetero-dimer of primers. The optimal primers were ordered from IDT (https://www.idtdna.com).

2.5 Cloning of JA and ET biosynthesis and signalling cDNAs

We used the cDNA synthesized from RNA of tissues as templates and the cloning primers that we designed to amplify *PcLOX, PcAOS*, *PcJAZ*, *PcACO* and *PcACS* by polymerase chain reaction (PCR). The PCR program was performed in a 50 ml reaction volume and consisting of 40 uL nuclease free water, 5 uL 10X amplification buffer, 1 uL deoxynucleoside triphosphates (dNTP), 1 uL forward primer, 1 uL reverse primer, 1 uL Taq polymerase, 2 uL template, these quantities are based off the NEB Standard Taq Protocol (M0273). PCR was carried out in a thermocycler (Biorad). The thermal cycle that was used for amplification was 30 seconds at 95℃ as initial denaturation, followed by 35 cycles of 30 sec at 95℃ for denaturation, 30 sec at 57 ℃ as annealing, 1 min 30 sec at 68 ℃ for extension, and final extension at 68 ℃ for 5 min. PCR products were examined by electrophoresis at 60 V for 1 hour in a 1% (w/v) agarose gel containing SYBR™safe in 0.5 x TBE buffer. A 1kb DNA ladder (NEB) was included on every gel. Electrophoresis gel was visualized in UV light.

The PCR products were purified by PCR Purification Kit (GeneJET PCR Purification Kit, Thermo, #K0702) and ligated to pGEM®-T Easy Vector (Promega) with T4 DNA ligase. Afterwards, the ligations were transformed into *E. coli* JM109 High Efficiency Competent Cells (Cat. #L2001) via heat-shock for 40 seconds in a water bath at 42℃. Cells were then incubated in Lysogeny broth (LB) medium at 37℃ for 1 hour before plating on LB plates with 50mg/mL of X-Gal and 100µg/mL of ampicillin . Plates were incubated overnight at 37 ℃ to conduct white / blue colony selection. White colonies were picked and run colony PCR to identifycolonies harboring inserts corresponding in size to the target gene. The positive colonies were streaked onto LB/Amp/X-Gal plates, and single colonies from these plates used to prepare 6 mL of liquid cultures in LB medium for plasmid purification (GeneJET Plasmid Miniprep Kit, Thermo, #K0503). For the next step, the plasmids were quantified with Nanodrop 1000 (Thermo Scientific, ON, Canada). Plasmids were used to create a dilution series to generate standard curves representing each gene for qRT-PCR. We also sequenced each cloned cDNA by Sanger sequencing (Molecular Biology Service Unit, University of Alberta), and used these sequences to design qRT-PCR primers as described above.

2.6 Quantification of Gene Expression using qRT-PCR

The reference genes ubiquitin-conjugating enzyme 11 (*PcUBC11*; accession GT239443.1), vacuolar ATP synthase subunit A (*PcVHA-A;* accession GT257942.1) and ubiquitin-activating enzyme 1 (*PcUBA1;* accession GT229647.1) were chosen because they were previously shown to be expressed at relatively stable levels across all treatments (Fortier et al, 2024). The qRT-PCR primers of target genes and reference genes were tested via real-time PCRThe cDNA was

amplified in a 10 ml reaction volume and consisting of 2.5 uL cDNA, 2.5 uL primers and 5 µL SYBR Green master mix. The qRT-PCR was conducted by QuantStudio™ 6 Flex Real-Time PCR system (Life Technologies™). The QuantStudio™ Real-Time PCR software v1.0 (Life Technologies™) was used to calculate Ct values, i.e. how many cycles of DNA amplification were required for the fluorescence to exceed the baseline level of detection. The standard curve for each cDNA was used to determine the linear dynamic range and efficiency of the primers, and the melt curve was examined to confirm that the designed primers only amplified a single product, with minimal signal arising from primer dimers.

2.7 Statistical Analysis

All statistical analyses were performed with R v4.3.1 (R Core Team 2023) and RStudio v2023.09.1+494 (RStudio Team 2022). The R data was modeled with a generalized linear mixed model (GLMM) by using the lme4 package, formulated as follows: Normalized transcript abundance ~ Treatment * Timepoint + (1 | Tree _number), family = Gamma (link = log). The suitability of reference gene combinations for qRT-PCR was analyzed through GLMM. The reference gene expression data was modeled using a GLMM with the formula: Average transcript abundance of combination ~ Treatment * Timepoint + (1 | Tree_number), family = Gamma (link = log). Summary outputs of the Transcript abundance GLMM are presented in Appendix 1.

Generalized linear mixed models were assessed for conformity to the assumptions of normality and homogeneity of variance using the results of Shapiro-Wilk tests (Shapiro and Wilk 1965)

and Levene tests (Levene 1960). Post hoc comparisons were conducted by the emmeans package v1.8.9 (Lenth 2020) to identify significant differences between groups, and letters were assigned by the multcomp package v1.4-23 (Hothorn et al. 2008). All graphical representations were generated employing the ggplot2 v3.4.4 (Wickham 2016) and cowplot v1.1.1 (Wilke 2020) packages.

Chapter 3: Results

3.1 cDNA cloning and sequence characterization

JA biosynthesis genes of *PcLOX* and *PcAOS*, JA signaling gene of *PcJAZ* and ET biosynthesis genes of *PcACO* and *PcACS* were all successfully identified in the lodgepole pine Illumina master transcriptome developed from Illumina paired-end sequences as described in Peery et al. (2021) using loblolly pine cDNAs as the queries. The deduced amino acid sequences corresponding each of these candidate genes were aligned with amino acid sequences from *A. thaliana*, *P. glauca* and *P. taeda* using Geneious 2021.1.1 (https://www.geneious.com) and phylogenetic trees were constructed using IQ tree (http://www.iqtree.org) (Figure 3.1-3.5). *A. thaliana* sequences were included in the phylogenetic analyses because this model organism is well-studied, and can help elucidate the evolutionary relationships and functional similarities between it and lodgepole pine as a reference, while *P. glauca* and *P. taeda* sequences were included to represent coniferous species, allowing for a more focused comparison within gymnosperms. Based on the phylogenetic analyses, the contigs closely related to *A. thaliana* amino acid sequences were selected for cloning to potentially capture functionally similar *LOX* genes in lodgepole pine. A total of two primer pairs were designed for *PcACO*, one pair for *PcACO1* and another for *PcACO2*, as well as a single primer pair for each of the genes *PcAOS*, *PcACS*, *PcJAZ*, and *PcLOX* were used to successfully clone cDNA corresponding to each contig (Table 3.1). Pairwise comparisons between the sequenced cDNA clones and the original contig sequences yielded nucleotide-level identities exceeding 97% (Figure 3.6-3.11). The small degree of mismatch is presumed to represent allelic variation between the two sequences, since the

cDNAs were cloned from different genotypes of lodgepole pine than were used to generate the master transcriptome.

qRT-PCR primer properties were determined using OligoAnalyzer™ Tool (IDT), and are presented in Table 3.2. Melt curve analyses were used to assess target specificity for each primer pair. The melt curve analyses for the candidate genes *PcLOX*, *PcAOS*, *PcJAZ, PcACO1 and PcACO2*, as well as the reference genes *PcVHA-A*, *PcUBC11* and *PcUBA1* all exhibited a single peak, signifying robust primer specificity (Figure 3.12). The melt curve analysis for *PcACS* revealed some primer-dimer peaks that were mainly evident in low cDNA abundance samples. Some samples also showed a shift in the major peak, raising the possibility of an off-target amplicon. However, since the majority of the samples showed little or no primer-dimer amplification and a consistent major peak representing the target, the selected primer pair was considered the most suitable for the experiments, having been chosen after testing of 8 distinct primer pairs. Therefore, while acknowledging the limitations, the data obtained with this primer pair were considered the best available in this case and were used for subsequent analyses.

3.2 Transcript Abundance Profiling

In this study, a total of 143 samples were collected from mature lodgepole pines, encompassing the six treatments described in Materials and Methods, and sampled at two distinct time points per treatment. Secondary xylem and secondary phloem were sampled from each tree. Six biological replicates were included per treatment and time point, except for the mock-inoculated xylem at 7 dpi treatment, which had five replicates. The MPB-attack experiment was conducted

under conditions of natural MPB attack, using pheromone-containing baits to attract MPB to the trees. Trees were allowed to be attacked for one week (7 days) following detection of the first MPB attack, then wrapped in fine mesh to prevent further attacks. This is different than conventional pest-insect interaction experiments, in which insects are introduced to the plant on a single day. In these MPB experiments, 0 days post-wound (dpw) was defined as the day on which the mock-attack trees were treated. Therefore, the 1 dpw MPB-attacked trees were subjected to MPB attacks for a period spanning 1 to 7 days prior to sampling, and the 7 dpw MPB-attacked trees had been subject to MPB attack for a period spanning 8 to 14 days prior to sampling. The *G. clavigera* inoculation experiment was conducted slightly in advance of the MPB flight period to ensure that trees that were part of this experiment did not get attacked by MPB.

JA and its active form, JA-Ile, has been demonstrated to increase in conifer species in response to attack by necrotrophic pathogens herbivorous insects and mechanical wounding (Arango-Velez et al. 2016; Bürger & Chory 2019; Fortier et al. 2024). These studies lead us to predict upregulation in the expression of genes related to JA biosynthesis and signaling following attack by MPB or inoculation with the fungus *G. clavigera*. JA is also known to be upregulated by wounding (Ralph et al. 2006; Glauser et al. 2008). In the analysis of the results obtained by qRT-PCR, *PcLOX* showed significant increases in both phloem and xylem transcript abundance of MPB-attacked trees by 7 dpw relative to both unwounded controls and mock-attacked trees (Phloem: *PcLOX* 7 dpw - MPB vs mock z = -3.48, $p = 0.001$; Xylem: *PcLOX* 7 dpw - MPB vs mock z = −3.21, $p = 0.003$; Figure 3.13 A & G). A significant increase in transcript abundance was also observed in mock-attacked trees at 1 dpw in xylem (Xylem: *PcLOX* 1 dpw - mock vs control z =

−2.92, $p = 0.009$; Figure 3.13 G). In the *G. clavigera* inoculation experiment, *PcJAZ* showed no significant difference in phloem, but did show significantly increased expression in response to mock-inoculation in xylem at both 7 and 14 dpi. While *PcJAZ* expression levels were also elevated in *G. clavigera* inoculated samples at both 7 and 14 dpi, these increases were not statistically significant. In the MPB attack experiment, *PcJAZ* showed significantly increased transcript abundance in MPB-attacked trees relative to untreated controls by 7 dpw in phloem and xylem (Phloem: *PcJAZ* 7 dpw - MPB vs control z = -3.73, $p < 0.001$; Xylem: *PcJAZ* 7 dpw - MPB vs control z = -6.32, $p < 0.001$; Figure 3.13 B & H). *PcJAZ* transcript abundance in mock-attacked xylem samples was also significantly higher than untreated controls (Xylem: *PcJAZ* 1 dpw - mock vs control z = -2.54, $p = 0.029$; *PcJAZ* 7 dpw - mock vs control z = -3.23, $p < 0.003$; Figure 3.13 H). *PcJAZ* showed significant increases in transcript abundance in mock-inoculated xylem samples was also significantly higher than untreated control at both 7 dpi and 14 dpi (Xylem: *PcJAZ* 7 dpi - mock vs control z = -2.76, $p = 0.015$; *PcJAZ* 14 dpi - mock vs control z = -2. 43, $p = 0.041$; Figure 3.13 H). In contrast to *PcLOX* and *PcJAZ*, the expression levels of *PcAOS*, another gene involved in the JA pathway, did not show significant changes across treatments in either the *G. clavigera* inoculation or MPB attack experiment. (Figure 3.13 C & I).

ET, an signaling molecule implicated in plant defense against necrotrophic pathogens, prompts the investigation of whether *G. clavigera* contributes to the MPB's ability to overcome tree defenses during an attack. Establishing whether ET induction occurs only in response to a *G. clavigera* challenge and not during the MPB's attack phase is necessary. In the study of ET biosynthesis genes, post-inoculation with *G. clavigera*, there was a significant increase in the expression of *PcACO*. *PcACO1* upregulated significantly by the 7 dpi and 14 dpi in the

secondary phloem and by the 14 dpi in the secondary xylem relative to both unwounded controls and mock-inoculated trees (Phloem: *PcACO1* 7 dpi - *G. clavigera* vs mock z = -6.10, $p < 0.001$; *PcACO1* 14 dpi - *G. clavigera* vs mock z = -2.45, $p = 0.038$; Xylem: *PcACO1* 14 dpi - *G. clavigera* vs mock z = −2.36, $p = 0.048$; Figure 3.13 D & J). I also observed significantly increased expression of *PcACO1* at 7 dpw in the secondary phloem (Phloem: *PcACO1* 7 dpw - *G. clavigera* vs mock z = −2.94, $p = 0.009$; Figure 3.13 D), relative to mock-inoculated treatments. *PcACO2* increased significantly by the 7 dpi in both phloem and xylem (Phloem: *PcACO2* 7 dpi - *G. clavigera* vs mock z = -2.45, $p = 0.038$; Xylem: *PcACO2* 7 dpi - *G. clavigera* vs mock z = -2.44, $p = 0.038$; Figure 3.13 E & K), relative to both unwounded controls and mock-inoculated trees. *PcACS* expression levels were below the limit of reliable quantification using the standard curve method, so there is no statistical analyses were conducted for *PcACS*.

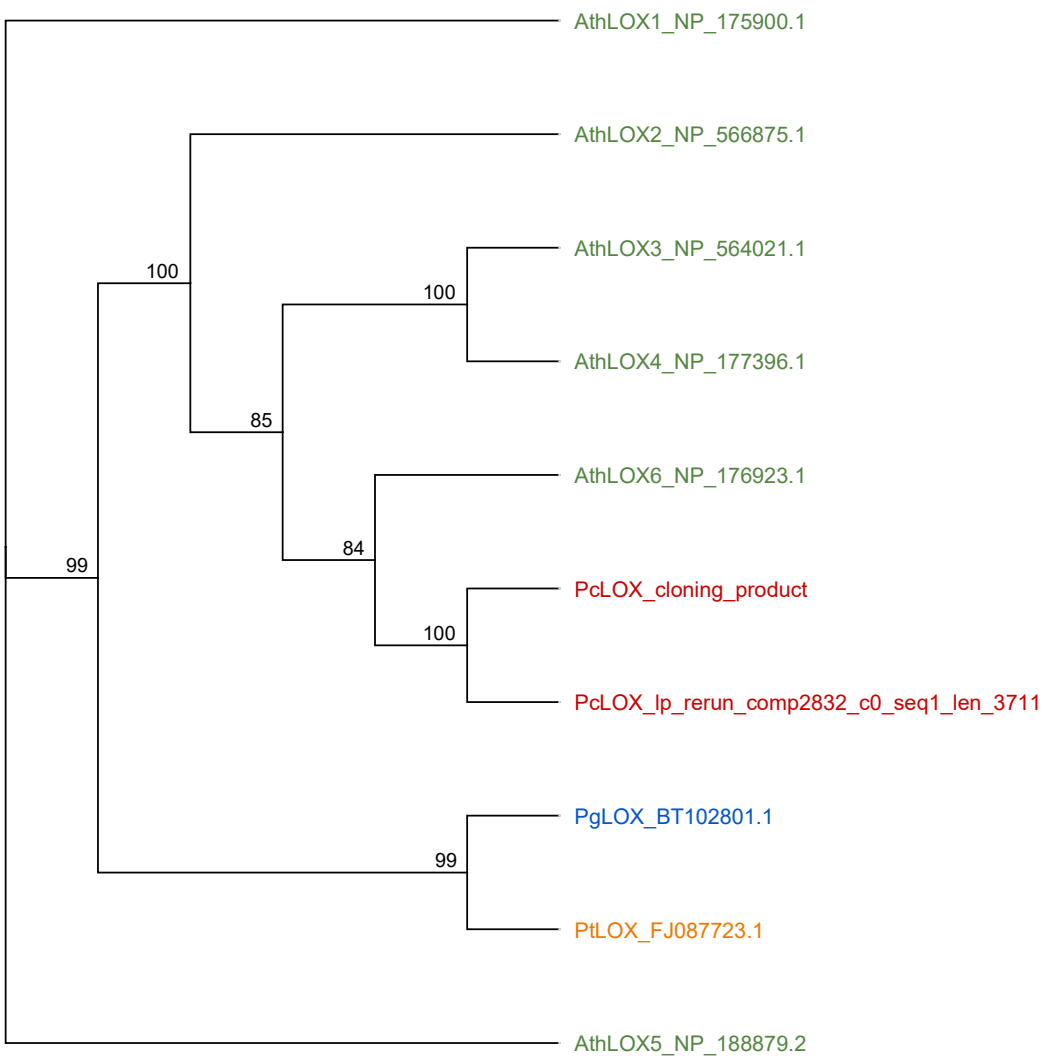

.

Figure 3.1: Phylogenetic trees constructed using maximum likelihood (ML) analysis, displaying the alignment of open reading frames (ORFs) sequences from *PcLOX* cloning product with amino acid sequences from *Arabidopsis thaliana* (*AthLOX*), *Picea glauca* (*PgLOX*), and *Pinus taeda* (*PtLOX*). Bootstrap values are shown at each node, providing statistical support for the phylogenetic inferences drawn. The specific contig of lp_rerun_comp2832_c0_seq1_len:3711 served as the cloning template within the *PcLOX* gene family.

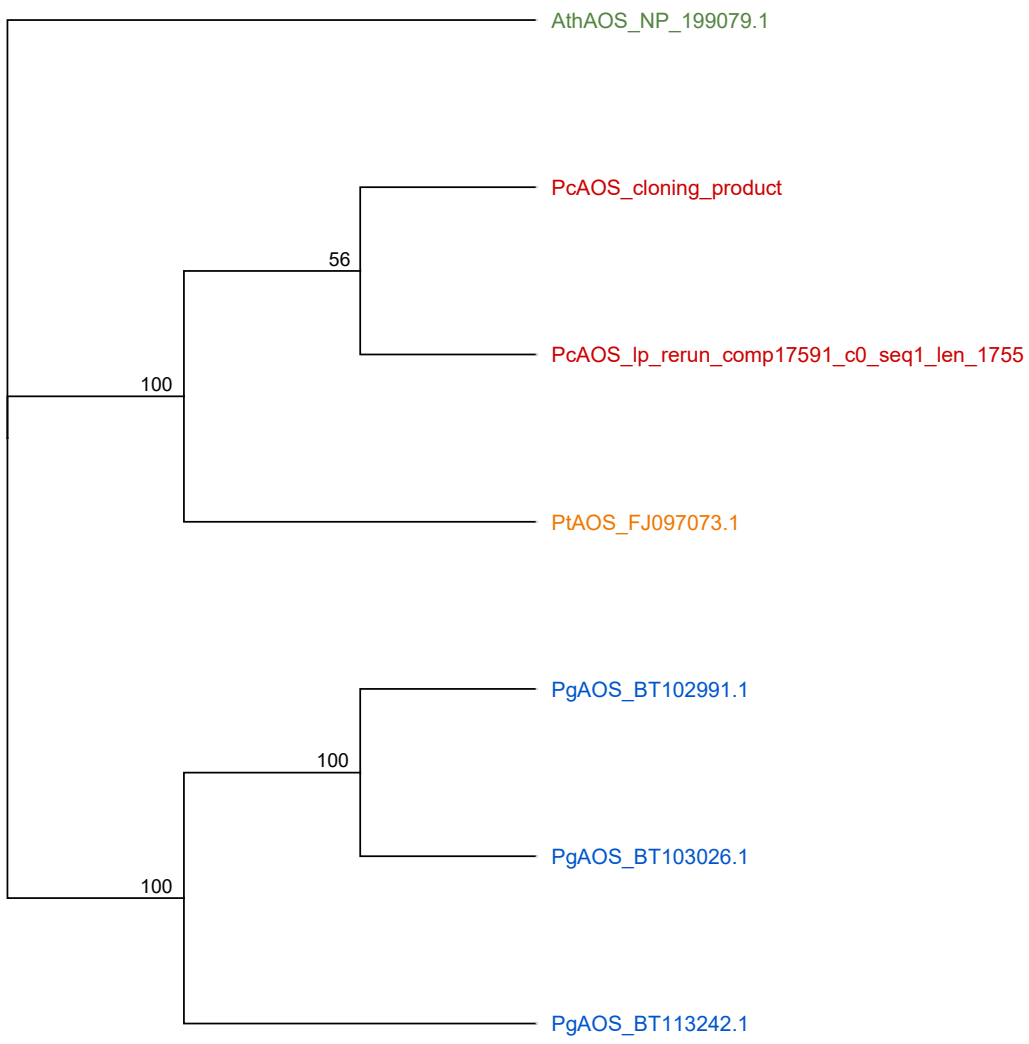

Figure 3.2: Phylogenetic trees constructed using maximum likelihood (ML) analysis, displaying the alignment of open reading frames (ORFs) sequences from *PcAOS* cloning product with amino acid sequences from *Arabidopsis thaliana* (*AthAOS*), *Picea glauca* (*PgAOS*), and *Pinus taeda* (*PtAOS*). Bootstrap values are shown at each node, providing statistical support for the phylogenetic inferences drawn. The specific contig of lp_rerun_comp17591_c0_seq1_len:1755 served as the cloning template within the *PcAOS* gene family.

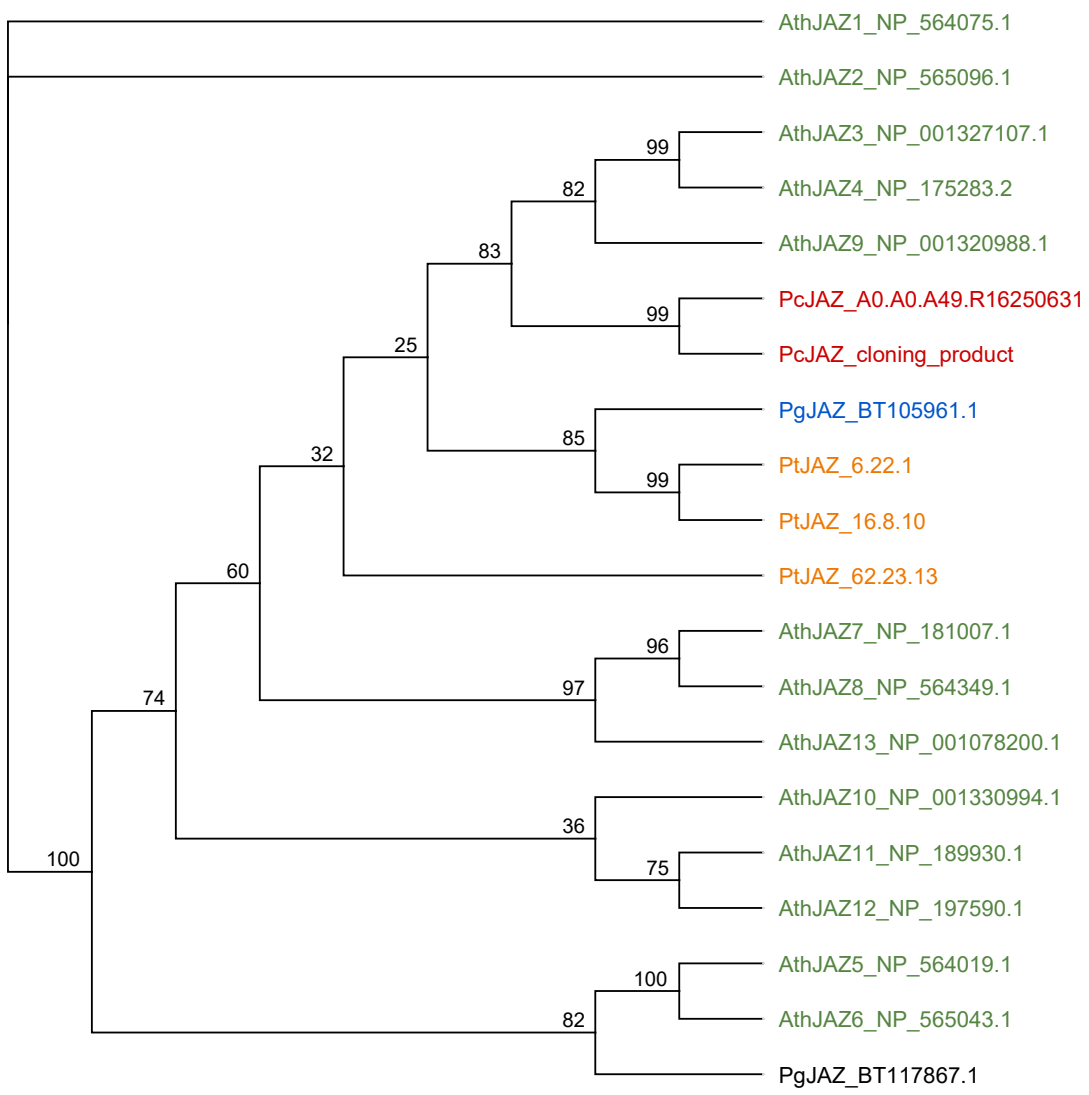

Figure 3.3: Phylogenetic trees constructed using maximum likelihood (ML) analysis, displaying the alignment of open reading frames (ORFs) sequences from *PcJAZ* cloning product with amino acid sequences from *Arabidopsis thaliana* (*AthJAZ*), *Picea glauca* (*PgJAZ*), and *Pinus taeda* (*PtJAZ*). Bootstrap values are shown at each node, providing statistical support for the phylogenetic inferences drawn. The specific contig of A0.A0.A49.R16250631 served as the cloning template within the *PcJAZ* gene family.

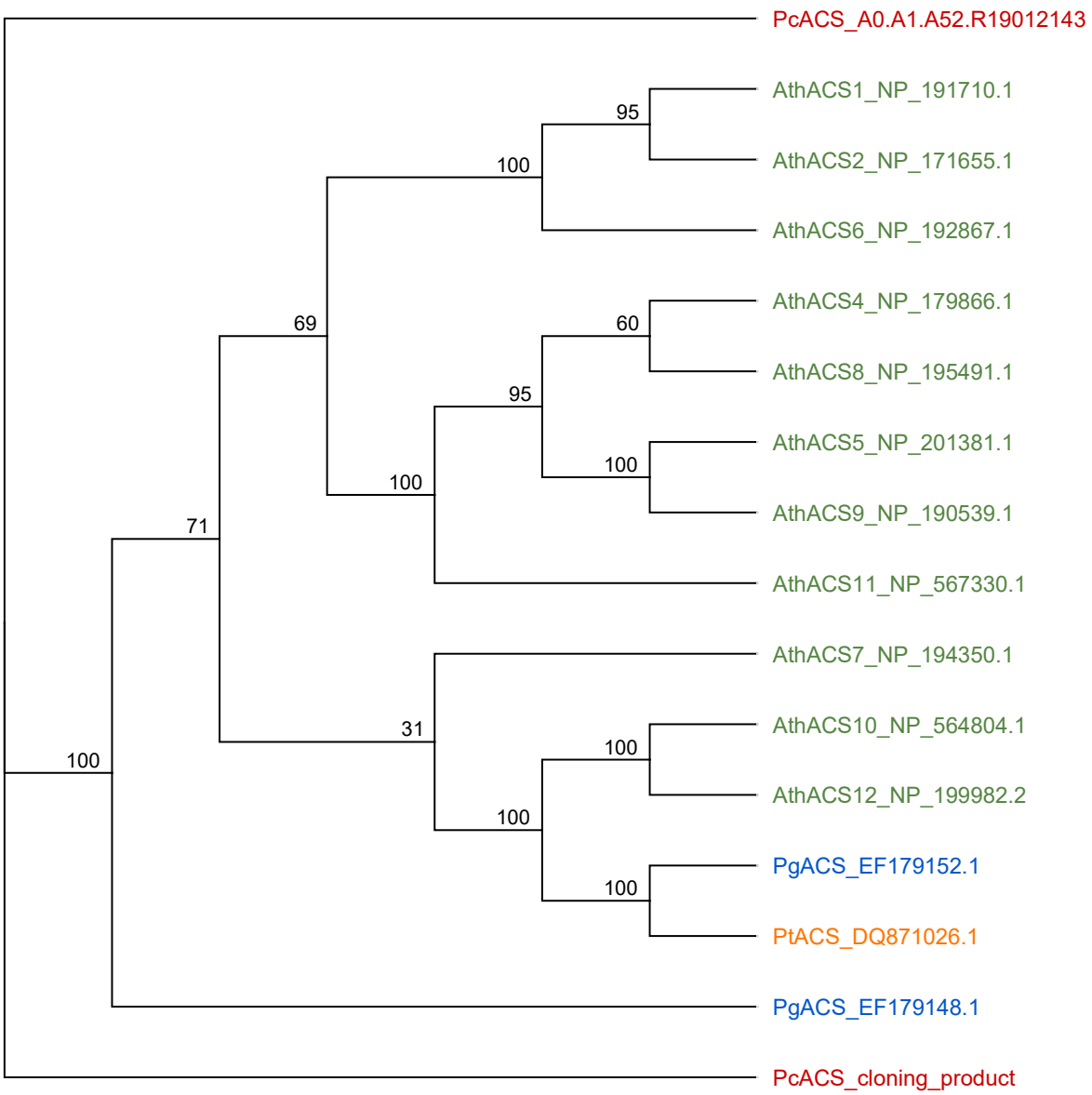

Figure 3.4: Phylogenetic trees constructed using maximum likelihood (ML) analysis, displaying the alignment of open reading frames (ORFs) sequences from *PcACS* cloning product with amino acid sequences from *Arabidopsis thaliana* (*AthACS*), *Picea glauca* (*PgACS*), and *Pinus taeda* (*PtACS*). Bootstrap values are shown at each node, providing statistical support for the phylogenetic inferences drawn. The specific contig of A0.A1.A52.R19012143 served as the cloning template within the *PcACS* gene family.

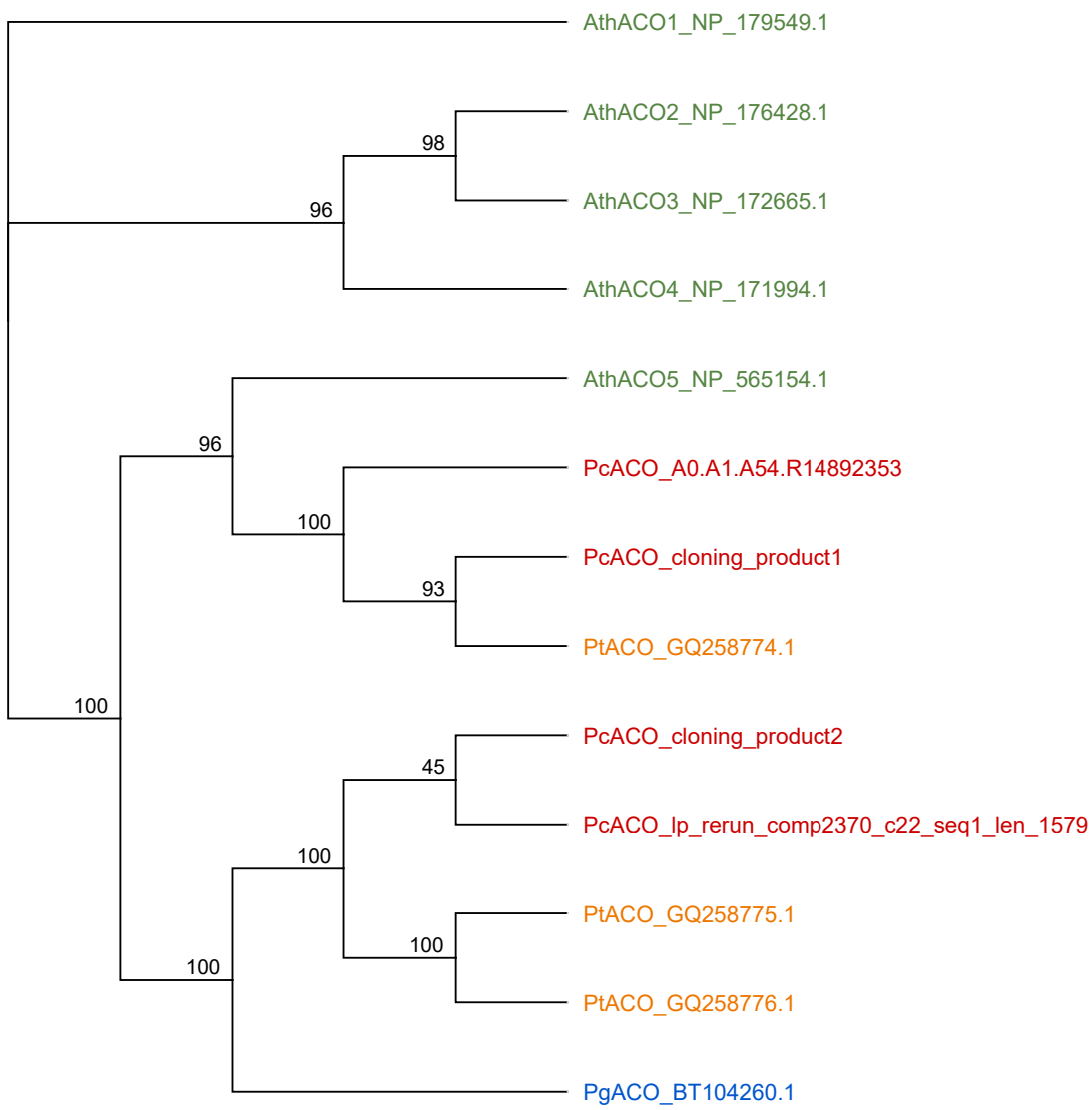

Figure 3.5: Phylogenetic trees constructed using maximum likelihood (ML) analysis, displaying the alignment of open reading frames (ORFs) sequences from *PcACO* cloning product with amino acid sequences from *Arabidopsis thaliana* (*AthACO*), *Picea glauca* (*PgACO*), and *Pinus taeda* (*PtACO*). Bootstrap values are shown at each node, providing statistical support for the phylogenetic inferences drawn. The specific contigs of A0.A1.A54.R14892353 and lp_rerun_comp2370_c22_seq1_len:1579 served as the cloning template within the *PcACO* gene family.

Table 3.1: Compilation of cloning primers utilized in the study. The table presents the primer sequences in conjunction with the corresponding contigs that were used as the basis for primer design in Geneious 2021.1.1 (https://www.geneious.com). Detailed information encompasses hairpin, homodimer, and heterodimer analysis, along with the melting temperature (Tm) and product size of the primers. All primers underwent rigorous PCR testing, culminating in the successful identification of two primer pairs for the *PcACO* groups, as well as a single primer pair for each of the genes *PcAOS*, *PcACS*, *PcJAZ* and *PcLOX*.

Gene	Primer Name	Primer Sequence	Hairpin	Homodimer	Heterodimer	Tm	Product Size	Contigs
PcLOX	LOX_1574_FWD2	TGCGTTGAGAGAGTGTCCAC	0.25	-3.61	-5.02	57.1	1629 bp	LOX-GROUP 2: lp_rerun_comp2832_c0_seq1_len:3711
	LOX_3367_REV2	TGGCCGTCCTCCTATGAAGA	-0.33	-9.28		57.7		
PcAOS	AOS_569_FWD2	TCAAGCGGTGGACTTGTGTT	-1.36	-5.5	-3.9	57.1	1420 bp	AOS-GROUP 1: lp_rerun_comp17591_c0_seq1_len:1755
	AOS_2041_REV2	AACGATGCGAGAGGAGGTTG	-0.61	-3.61		57.2		
PcJAZ	JAZ_3022_FWD5	TCTGCGCAGGGTGTTAAGAG	0.01	-16.99	-8.7	57.2	1551 bp	JAZ-GROUP 1: A0.A0.A49.R16250631
	JAZ_4724_REV5	AAACGCACCTGGTATGCAGA	-1.9	-7.05		57		
PcACS	ACS_131_FWD8	GGAATCACCCAGAGCAGCTT	-0.01	-6.34	-6.31	57.5	1444 bp	ACS-GROUP 1: A0.A1.A52.R19012143
	ACS_1547_REV8	ACATCGCTCATTCGATCCCC	-1.24	-6.76		57.2		
PcACO 1	ACO_2805_FWD2	GTGTTGTTGTTTGTGTGTGGG	2.5	None	-5.24	56.1	1212 bp	ACO-GROUP 1 A0.A1.A54.R14892353
	ACO_4874_REV2	TGCAGCAACCTGACCTAGAT	-1.43	-7.05		56.1		
PcACO 2	ACO_2851_FWD2	GCAGTCCCCGTGATTGACAT	-0.64	-3.61	-7.71	57.7	1243 bp	ACO-GROUP 2: lp_rerun_comp2370_c22_seq1_len:1579
	ACO_4954_REV2	CGCTTACTGGGAAGTGGAGA	-2	-3.61		56.5		

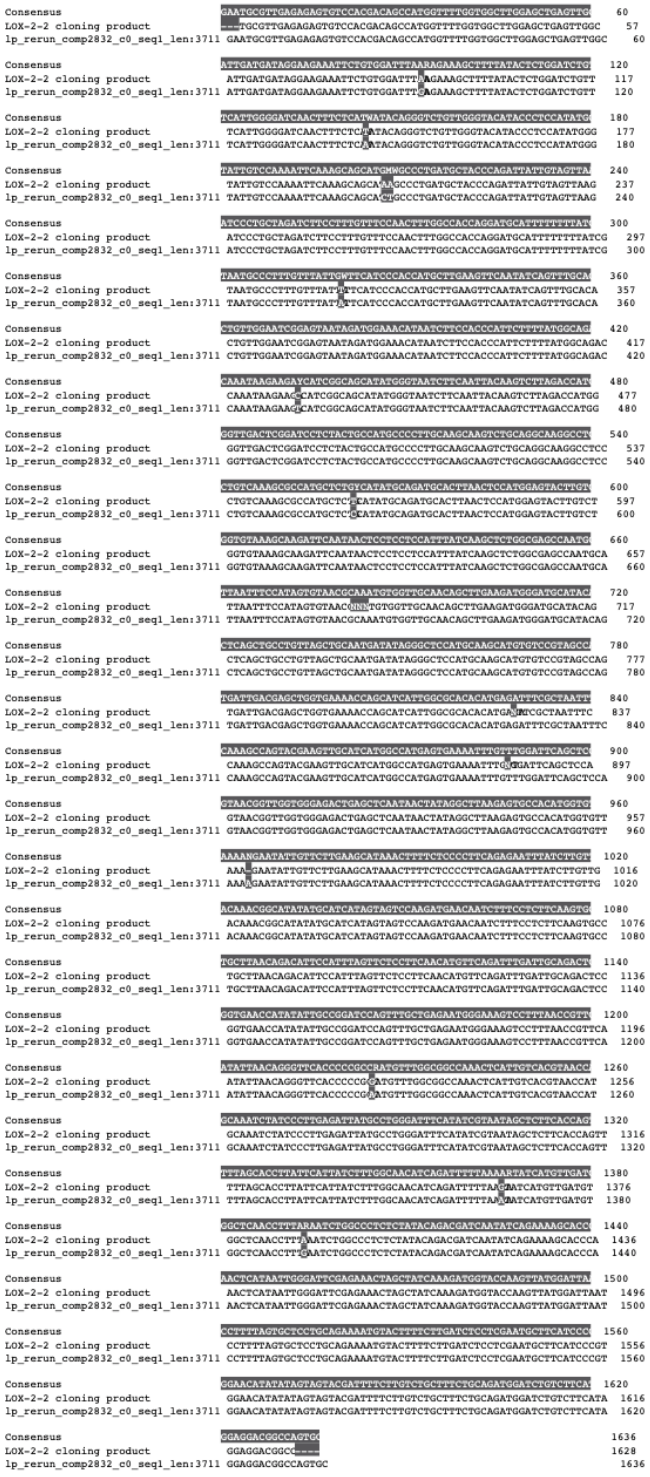

Figure 3.6: Alignment of the cloned *PcLOX* cDNA sequence with the original sequence from the lodgepole pine master transcriptome, revealing a pairwise identity of 99.1%. The high degree of nucleotide identity between the contig and the cloned cDNA product indicates successful cloning of this cDNA for use in qRT-PCR.

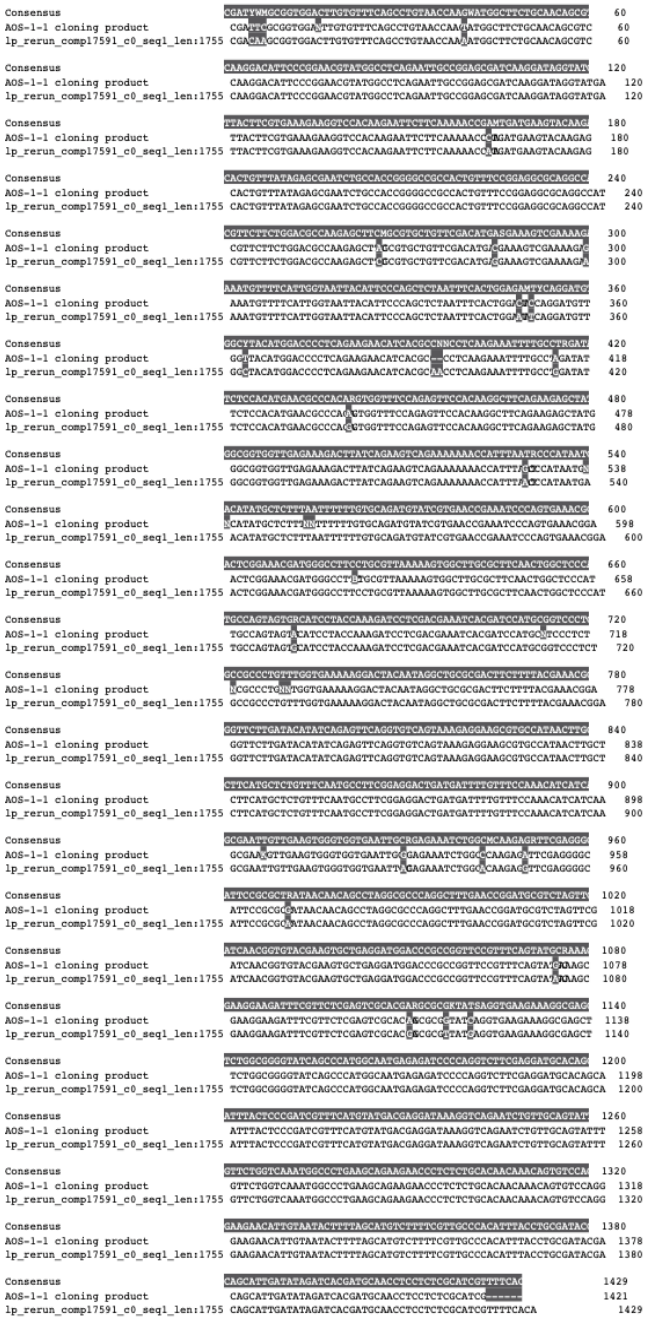

Figure 3.7: Alignment of the cloned *PcAOS* cDNA sequence with the original sequence from the lodgepole pine master transcriptome, revealing a pairwise identity of 97.7%. The high degree of nucleotide identity between the contig and the cloned cDNA product indicates successful cloning of this cDNA for use in qRT-PCR.

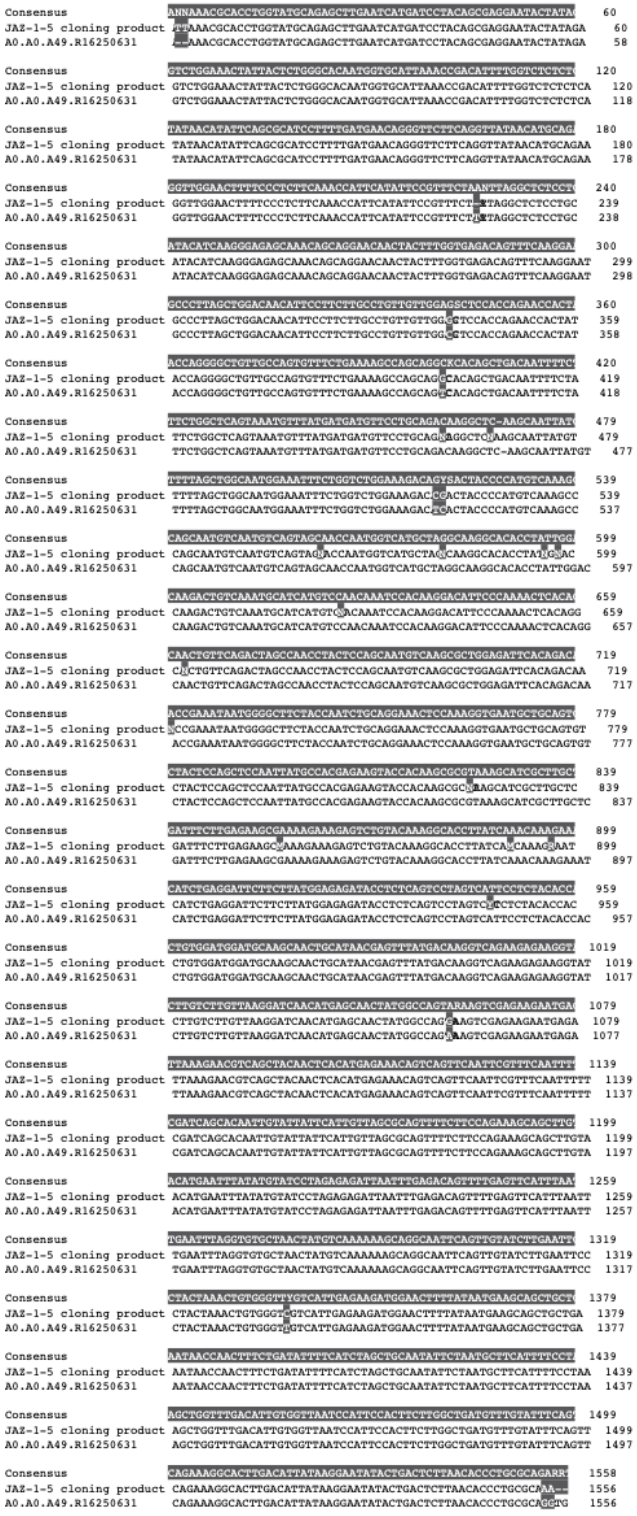

Figure 3.8: Alignment of the cloned *PcJAZ* cDNA sequence with the original sequence from the lodgepole pine master transcriptome, revealing a pairwise identity of 98.7%. The high degree of nucleotide identity between the contig and the cloned cDNA product indicates successful cloning of this cDNA for use in qRT-PCR.

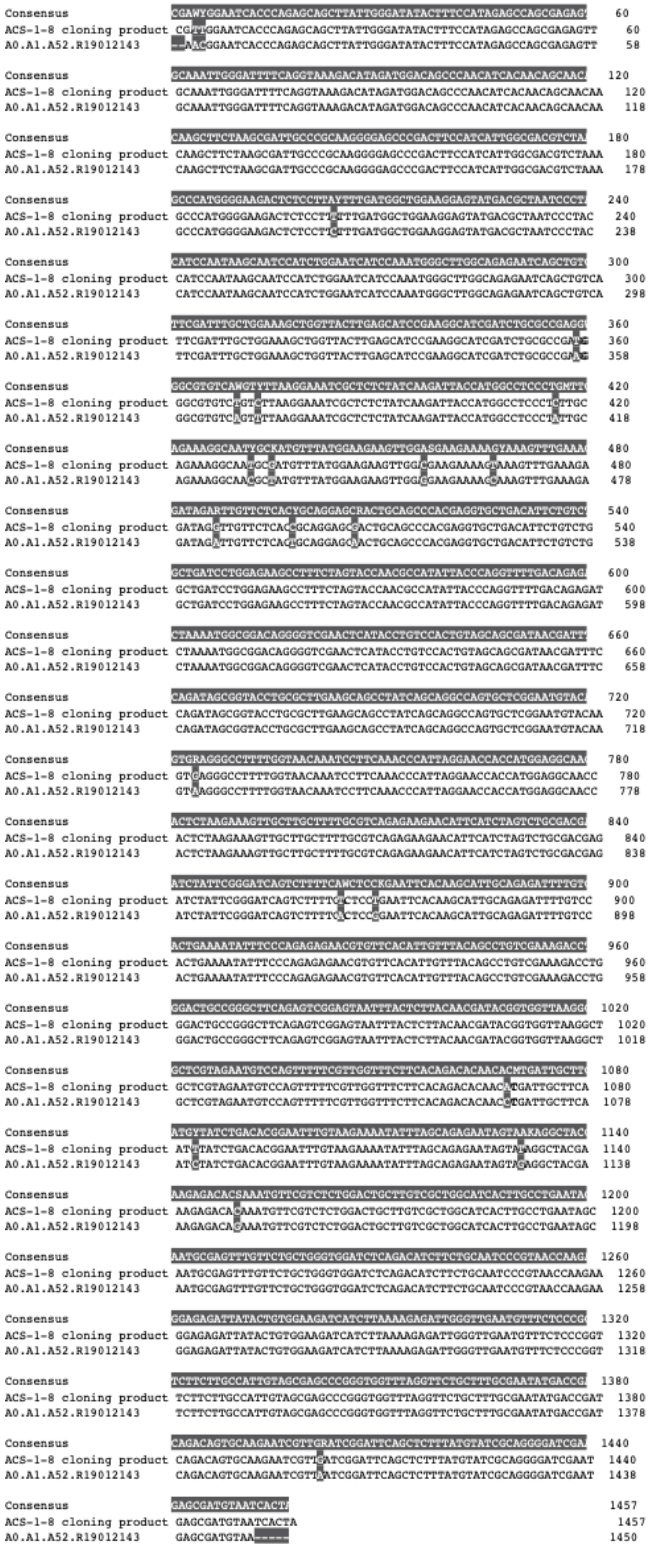

Figure 3.9: Alignment of the cloned *PcACS* cDNA sequence with the original sequence from the lodgepole pine master transcriptome, revealing a pairwise identity of 98.5%. The high degree of nucleotide identity between the contig and the cloned cDNA product indicates successful cloning of this cDNA for use in qRT-PCR.

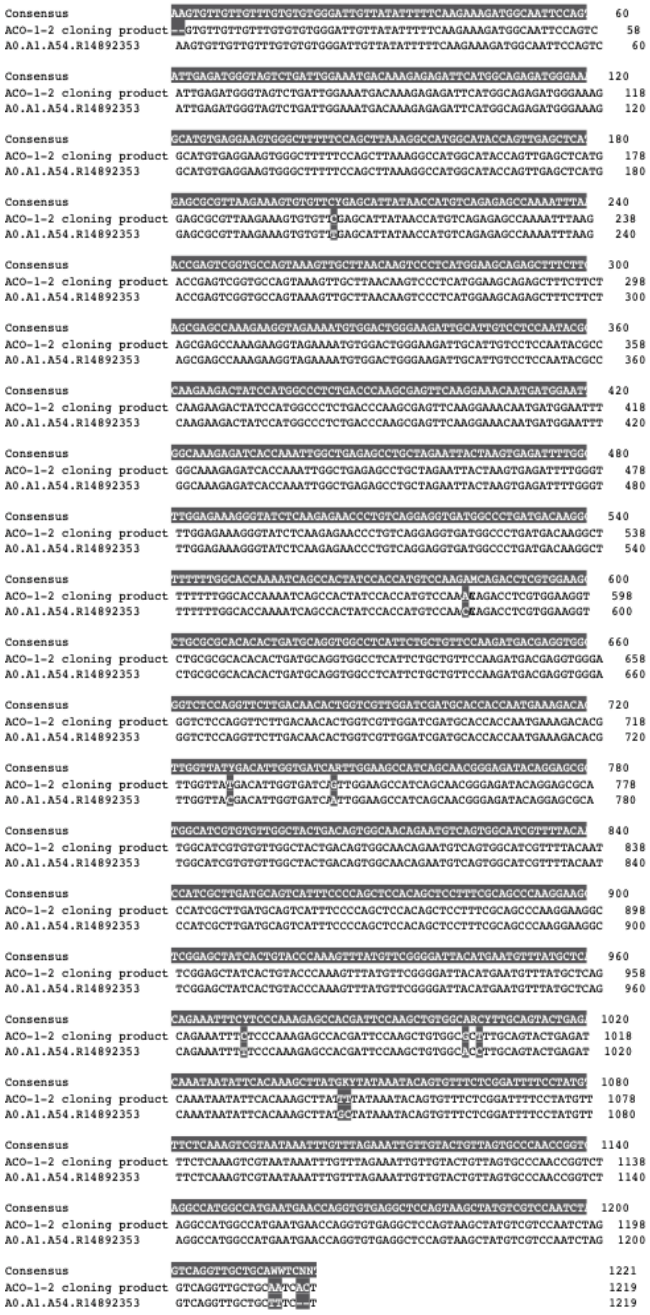

Figure 3.10: Alignment of the cloned *PcACO 1* cDNA sequence with the original sequence from the lodgepole pine master transcriptome, revealing a pairwise identity of 98.9%. The high degree of nucleotide identity between the contig and the cloned cDNA product indicates successful cloning of this cDNA for use in qRT-PCR.

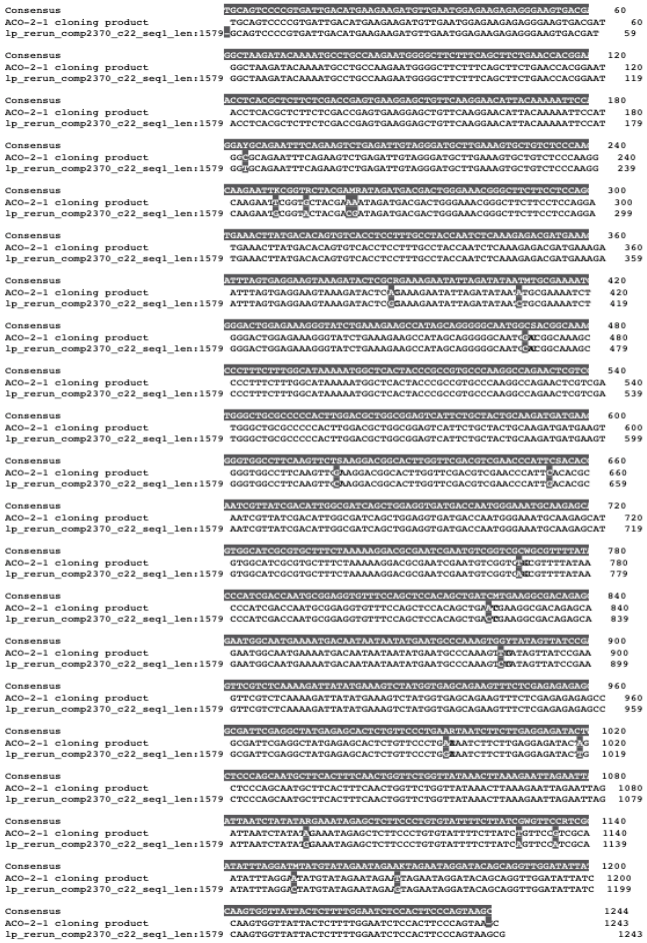

Figure 3.11: Alignment of the cloned *PcACO 2* cDNA sequence with the original sequence from the lodgepole pine master transcriptome, revealing a pairwise identity of 98.4%. The high degree of nucleotide identity between the contig and the cloned cDNA product indicates successful cloning of this cDNA for use in qRT-PCR.

Table 3.2: Compilation of qRT-PCR primers employed in the study. The table provides comprehensive details, including hairpin, homodimer, and heterodimer analysis, as well as the melting temperature (Tm) and product size of the primers.

Gene	Prime name	Primer sequence	GC	Tm	Hairpin	Homodimer	Heterodimer	Product size
PcLOX	LOX-266-F1	CCAACTTTGGCCACCAGGAT	55	58.1	-1.1	-13.19	-6.97	109bp
	LOX-374-R1	TCCGATTCCAACAGTGTGCA	50	56.9	0.55	-7.05		
PcAOS	AOS-741-F1	AGGACTACAATAGGCTGCGC	55	57.1	-0.21	-9.89	-6.75	102bp
	AOS-842-R1	AGAGCAAGTTATGGCACGCT	50	57.1	-0.44	-4.74		
PcJAZ	JAZ-1088-F2	ACGTCAGCTACAACTCACATGA	45.5	56.1	0.04	-6.34	-4.74	100bp
	JAZ-1187-R2	CTGGAAGAAAACTGCGCTAACA	45.5	55.7	0.49	-9.89		
PcACS	ACS-832-F6	TGCGACGAGATCTATTCGGG	55	56.5	-1.28	-7.82	-5.19	129bp
	ACS-960-R6	CAGGTCTTTCGACAGGCTGT	55	57.2	-1.33	-6.76		
PcACO 1	ACO-751-F1	GCCATCAGCAACGGGAGATA	55	57.2	-0.75	-3.61	-6.69	125bp
	ACO-875-R1	TGTGGAGCTGGGGAAATGAC	55	57.4	0.98	-6.34		
PcACO 2	ACO-668-F1	ATCGACATTGGCGATCAGCT	50	56.9	-1.25	-6.76	-8.33	96bp
	ACO-763-R1	CGACATTCGATTCGCGTCCT	55	57.6	-0.99	-10.36		

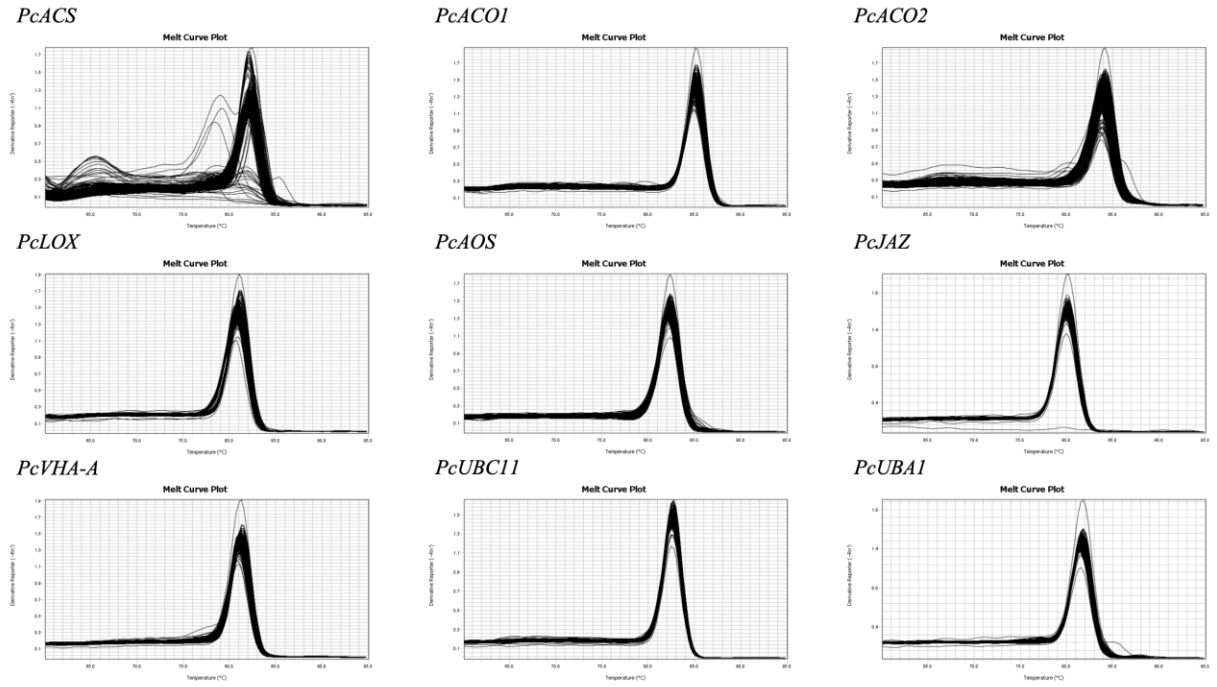

Figure 3.12: Melt curve analysis of qRT-PCR. Melting curve analyses provide a means to test whether the primers used in the assay produce a single amplicon product during real-time PCR, and also whether the primers generate measurable amounts of primer dimers. Data represent the negative of the first derivative of the fluorescence obtained as the temperature is raised from 80°C to 85°C. The melt curves of the target genes *PcLOX*, *PcAOS*, *PcJAZ*, *PcACO1* and *PcACO2*, along with the reference genes *PcVHA-A*, *PcUBC11* and *PcUBA1*, all display a single peak and smooth baseline, indicative of robust primer specificity and limited or no primer dimers. The melt curves for some samples for *PcACS* exhibit multiple and/or shifted peaks, suggesting that these primers have lower efficiency than the other primers, and that primer dimers and other products are resulting when target template is low.

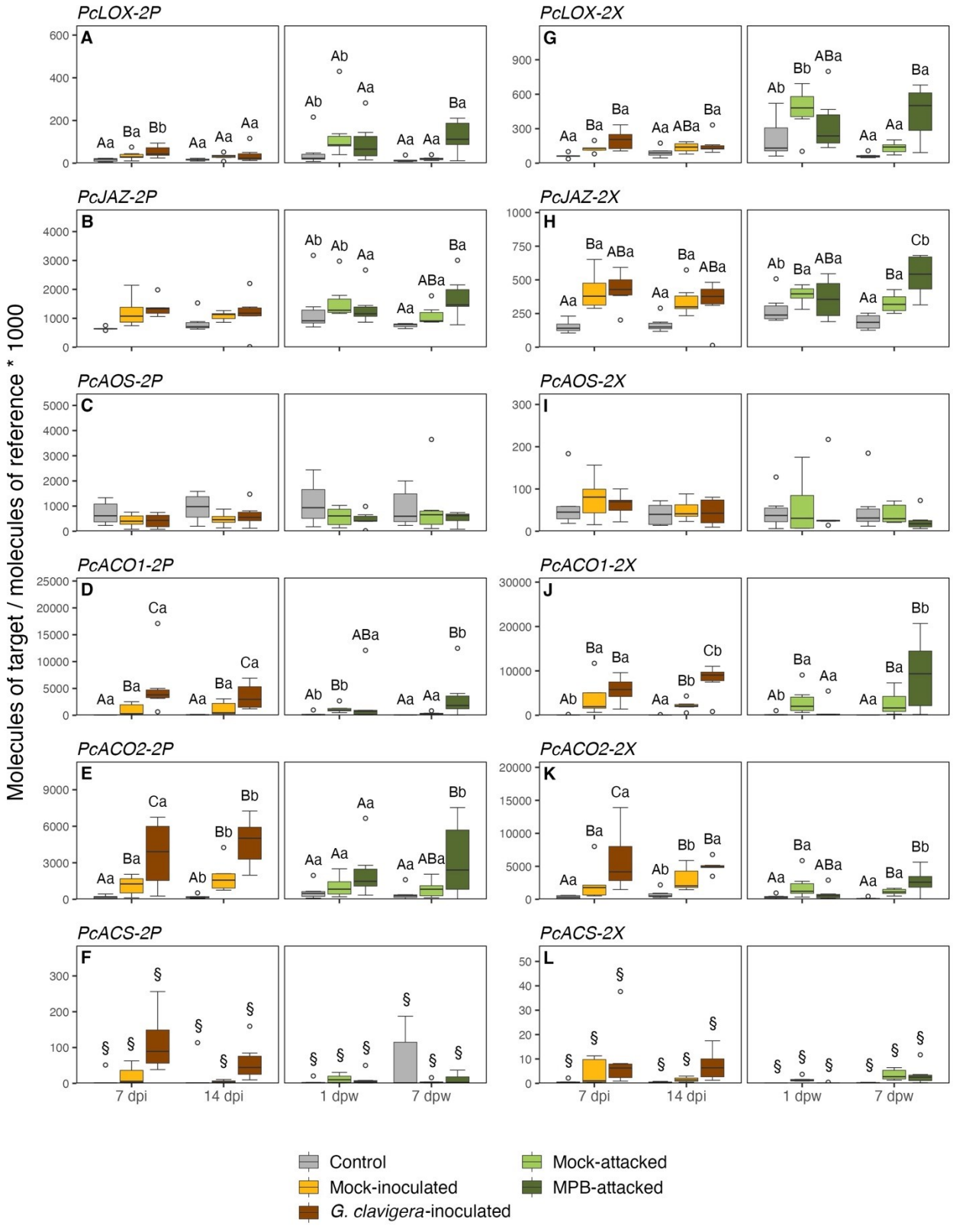
PcLOX-2P
PcLOX-2X
PcJAZ-2P
PcJAZ-2X
PcAOS-2P
PcAOS-2X
PcACO1-2P
PcACO1-2X
PcACO2-2P
PcACO2-2X
PcACS-2P
PcACS-2X
Molecules of target / molecules of reference * 1000
7 dpi
14 dpi
1 dpw
7 dpw
Control
Mock-inoculated
G. clavigera-inoculated
Mock-attacked
MPB-attacked

Figure 3.13: Transcript abundance as measured by qRT-PCR for JA biosynthesis and signaling genes and ET biosynthesis genes in *G. clavigera*-inoculated or MPB-attacked lodgepole pine trees. Secondary phloem (A-F) and secondary xylem (G-M) were harvested from lodgepole pine that were inoculated with *G. clavigera* at 7 or 14 days post inoculation (dpi), mock-inoculated or untreated control (A, C, E, G, I, K), or from lodgepole pine that were mass-attacked by MPB at 1 or 7 days post wounding (dpw), mock-attacked or untreated control (B, D, F, H, J, L). (A) lipoxygenase (*PcLOX*) in phloem, (B) jasmonate-zim domain (*PcJAZ*) in phloem, (C) allene oxide synthase (*PcAOS*) in phloem, (D) 1-aminocyclopropane-1-carboxylate oxidases (*PcACO1*) in phloem, (E) 1-aminocyclopropane-1-carboxylate oxidases (*PcACO2*) in phloem, (F) 1-aminocyclopropane-1-carboxylic acid synthase (*PcACS*) in phloem, (G) lipoxygenase (*PcLOX*) in xylem, (H) jasmonate-zim domain (*PcJAZ*) in xylem, (I) allene oxide synthase (*PcAOS*) in xylem, (J) 1-aminocyclopropane-1-carboxylate oxidases (*PcACO1*) in xylem, (K) 1-aminocyclopropane-1-carboxylate oxidases (*PcACO2*) in xylem, (L) 1-aminocyclopropane-1-carboxylic acid synthase (*PcACS*) in xylem. Boxplots represent a §. Uppercase letters indicate significant differences between treatments within a time point; lowercase letters indicate significant differences between estimated marginal means of a treatment between time points (Tukey-adjusted p-value < 0.05, n = 5-6). There are no letters assigned for *PcAOS* because no significant difference was observed in *PcAOS* transcript abundance profiles between treatments. *PcACS* expression levels were below the limit of reliable quantification using the standard curve method, and as such are marked with a §. Because *PcACS* transcript abundance values were below the limit of reliable quantification, no statistical analyses were conducted for *PcACS*.

Chapter 4: Discussion

To ascertain the potential significance of ophiostomatoid fungal symbionts associated with the mountain pine beetle in contributing to the beetle's ability to overcome lodgepole pine defenses during the mass attack phase, we conducted a comparative analysis between the tree's response to natural MPB attack and its response to inoculation with the necrotrophic fungal associate *G. clavigera*. *G. clavigera* was chosen for its status as one of the most common fungal associates of the MPB (Lee et al. 2006; Roe, James, et al. 2011) and its distinction as the earliest and fastest colonizer among the common ophiostomatoid fungal associates (Solheim 1995; Solheim & Krokene 1998). Furthermore, *G. clavigera* has demonstrated sufficient virulence to cause pine mortality in the absence of MPB (Owen et al. 1987; Yamaoka et al. 1995). In this study, I employed qRT-PCR transcript abundance profiling to meticulously assess the expression patterns of genes involved in the biosynthesis and signaling pathways of JA and ET in lodgepole pine. Arango-Velez et al. (2016) have demonstrated JA is able to activate lodgepole pine's responses against necrotrophic pathogens like *G. clavigera* and herbivorous insects such as MPB. Furthermore, *G. clavigera*, acting as a necrotrophic fungal pathogen, exhibits the capability to induce the synthesis of ET (Fortier et al. 2024; Dong 1998).

If the ophiostomatoid fungi do not significantly contribute to the MPB's ability to overcome tree defenses during a mass attack, then it is likely that these fungi serve alternative function that provide some benefit to MPB fitness during subsequent colonization by the attacking MPB and their offspring. Ophiostomatoid fungi are highly specific obligate mutualists essential for the growth and survival of bark beetles (Six 2012). In these obligate mutualistic relationships, the

fungi contribute vital nutrients to the beetles, and in return, the beetles serve as a means of transportation for the fungi to find a suitable host tree. (Ayres et al. 2000; Bentz and Six 2006; Bleiker and Six 2007; Six and Elser 2019). The challenge for fungi and beetles lies in the difficulty of digesting the lignin and cellulose present in bark and sapwood, when easily utilized carbohydrates are quickly consumed, the larvae and fungi require additional nutrients for growth (Six 2020a). Fungi play a crucial role by acquiring carbon from tree defenses and making it accessible to beetles, thereby mitigating the challenges posed by intra-specific competition arising from mass attacks (Zhao et al. 2018; Wang et al. 2013; Zhou et al. 2016).

In the investigation of the expression patterns of JA biosynthesis and signaling genes in response to MPB mass-attack and *G. clavigera* inoculation, the gene *PcLOX* exhibited significant upregulation relative to unwounded control, and the gene *PcJAZ* increased significantly in response to *G. clavigera* in the xylem and to MPB in the phloem, relative to the unwounded control. These observations are consistent with model that JA response, typically associated with defense against necrotrophic pathogens and insects, would be triggered following both MPB and *G. clavigera* challenges. The mock treatments also led to an upregulation of gene expression relative to untreated controls. As a result, the differences between mock and *G. clavigera* or MPB treatments did not reach statistical significance. One potential explanation for the upregulation in mock treatments is the induction of JA response by mechanical wounding. In our experiment, each of the mock-treated trees underwent deliberate wounding, with 6-8 1/2-inch round holes penetrating the bark through to the cambium. Previous studies have demonstrated that wounding can induce an increase in JA levels, as evidenced in *A. thaliana* (Glauser et al.

2008). Moreover, in conifers, the induction of JA biosynthesis genes, such as *LOX* and *AOS* transcripts, has been observed in response to wounding (Ralph et al. 2006).

Additionally, the observed significant increase in *PcLOX* transcript abundance in response to *G. clavigera*, relative to the unwounded control, in both phloem and xylem tissues underscores a differential temporal expression pattern between these two tissue types. Notably, the increase in the phloem was detected only at the early time point, whereas in the xylem, elevated transcript levels were observed at both early and late time points. This pattern aligns with the theoretical model and suggests a more ephemeral, or short-term, expression of *PcLOX* in the phloem compared to a sustained response in the xylem. Such findings are logical when considering the pathogenic behavior of *G. clavigera*, which is believed to colonize the xylem more extensively than the phloem (Bleiker & Six 2007).

In examining the transcript abundance of *PcAOS* across various treatments, we observed no statistically significant differences. It indicates that this enzyme may not be upregulated in the synthesis of JA; it is possible that the existing levels of the enzyme are adequate for JA synthesis and, suggesting that *PcAOS* is not a rate-limiting factor in this pathway. Alternatively, the actual enzyme responsible for JA synthesis in these tissues might be a different, upregulated member of the AOS gene family. This result prompts us to explore alternative genes within the *AOS* family for further research. Although the *AOS* gene family exhibits structural conservation, it also displays diverse evolutionary mechanisms in different plant species. Notably, several plants including *A. thaliana*, possess multiple *AOS* genes (Laudert et al. 1996; Howe et al. 2000; Maucher et al. 2000). The diversity within the *AOS* gene family is further reflected in the

clustering of AOSs from different plant species into four groups: 13-AOS, 9-AOS, 9/13-AOS type I, and 9/13-AOS type II. This functional differentiation is crucial, as it has been demonstrated that not all AOS proteins can participate in JA synthesis (Sun, 2022). In contrast, the JAZ family, which plays a pivotal role in JA signaling, exhibits greater diversity in terms of gene expression. In Arabidopsis, 13 JAZ genes are expressed. Distinct *JAZ* genes may exhibit variations in their responses to JA and other signaling molecules. For instance, *JAZ13* lacks a TIFY domain that facilitates interactions like JAZ-JAZ interactions (Thireault et al. 2015; Chung and Howe 2009). *JAZ7* and *JAZ8* possess non-functional Jas degron sequences, resulting in weak binding to COI1 and resistance to degradation by the 26 S proteasome (Shyu et al. 2012). In summary, the diversity among AOS and JAZ genes is not only numerical but extends to the structural and functional levels. Identifying more genes from *PcAOS* and *PcJAZ* families helps us understand the biosynthesis and signaling pathway in JA response to MPB attack versus *G. clavigera* inoculation.

Given that *PcACS* transcript abundance values fell below the threshold for reliable quantification, statistical analyses concerning *PcACS* were not conducted. This scenario may hint at the possibility that the actual enzyme pivotal for JA synthesis in the examined tissues might not be the *PcACS* that I identified but rather another upregulated isoform within the ACS gene family. The ACS gene, known to be encoded by a small gene family across all plant species, exhibits considerable diversity. For example, in Arabidopsis, nine ACS isoforms have been identified, categorized based on their C-terminal sequences into three types: type I (ACS1, ACS2, and ACS6), type II (ACS4, ACS5, ACS8, ACS9, and ACS11), and type III (ACS7) (Yoshida et al. 2005). This classification underscores the nuanced regulation of ACS protein

activity across multiple levels, a domain where much remains to be uncovered, particularly concerning the specific roles of ACS isoforms in ethylene induction following certain stimuli and the overarching regulatory mechanisms, especially in conifers.

The intricate regulation of ACS, combined with the observed trend of *PcACS* transcript upregulation in response to *G. clavigera* challenges, despite falling below quantification limits, posits a complex interaction network. It suggests that increasing the cDNA template concentration might yield quantifiable results, potentially unlocking insights into the specific contributions of *PcACS* isoforms to ethylene biosynthesis in response to biotic stress.

The expression patterns of *PcACO1* and *PcACO2* are notably similar, and following *G. clavigera* inoculation, we observed a significant increase in both *PcACO1* and *PcACO2* transcripts abundance relative to unwounded controls and mocks. This is in line with the model suggesting that *G. clavigera*, as a necrotrophic fungal pathogen, can induce ethylene (ET) synthesis, supporting findings by Fortier et al. (2024). However, it is after MPB attack that we see a significant rise in *PcACO1* and *PcACO2* levels relative to the unwounded control, but only at a later time point in both phloem and xylem tissues. This delayed response might indicate the plant's initial reaction to MPB-vectored *G. clavigera*, as the significant changes were only detected later in the attack phase, suggesting that *G. clavigera* colonization might be enough to prompt the plant's perception of the fungal pathogen at this point, as MPB transitions from the mass-attack phase to the colonization phase. Alternatively, this could also reflect the JA-mediated upregulation of ET that happens through the wounding effect of MPB. There is evidence that the intrusion of bark by these pests prompts the release of jasmonates, which in

turn activate the production of ACO and ET in specific plant tissues such as ray parenchyma, cambium, and the epithelia of resin ducts (Hudgins & Franceschi 2004).

The other explanation of *PcACO1* and *PcACO2* increasing after MPB attack is a secondary response stemming from the wounding caused by MPB. Across most wounding treatments, we consistently found significant increases in gene expression. It is well-documented that wounding triggers the formation of traumatic resin ducts, a process involving ethylene signaling (Heyman et al. 2018). Given that wounding also elevates JA levels, it is plausible to surmise that JA might play a role in amplifying ET gene expression, forming a complex interplay between these two phytohormones in the plant defense response (Bürger & Chory 2019; Erb & Reymond 2019). ET has also been recently implicated in plant repair responses (Heyman et al. 2018). These transcript profiling experiments reveal an additional layer of complexity in the roles for ET in host responses to MPB attack that require additional experiments to resolve.

Chapter 5: Conclusion

My thesis project seeks to investigate the expression of genes linked to the biosynthesis and signaling of JA and ethylene ET in lodgepole pine, using qRT-PCR to analyze samples from trees either attacked by the MPB or infected with *G. clavigera*. This research provides insight into whether *G. clavigera* contributes to MPB's ability to breach the tree's defenses. By selecting key genes based on previous transcriptome analyses by the Cooke Lab, I focused on JA biosynthesis genes *PcLOX* and *PcAOS*, the JA signaling gene *PcJAZ*, and ET biosynthesis genes *PcACO* and *PcACS*.

The study has found that JA biosynthesis gene *PcLOX* is upregulated in trees attacked by MPB, inoculated with *G. clavigera*, and even in mock-treated trees, corroborating the idea that the JA pathway is activated in response to herbivorous insects, fungal pathogens, and physical damage. This gene expression pattern reflects the same pattern as the hormone steady state levels (Table 5.1). JA signaling gene *PcJAZ* is upregulated only during MPB attack, mirroring the hormone levels. However, its expression does not increase following *G. clavigera* inoculation, distinguishing it from the hormone response (Table 5.1).

Meanwhile, ET biosynthesis genes, *PcACO1* and *PcACO2*, showed significant upregulation following *G. clavigera* inoculation, reflecting in the elevated levels of the ET precursor ACC in these trees (Table 5.1). This upregulation was also noted in trees at later time point following the MPB attack (Table 5.1). The timing of ET gene expression suggests that the perception of fungal pathogens occurs as the tree transitions from mass attack to colonization, although it does not

immediately result in higher ACC levels. Alternatively, this increased ET gene expression may relate to the production of traumatic resin ducts or be part of the plant's repair processes. The complexity of ET's roles in the host response to MPB attack, demonstrated by these gene expression profiles, underscores the need for further experimental work to fully elucidate these defense mechanisms.

JA & ET biosynthesis gene *PcAOS* and *PcACS* do not show significant upregulations in their expression (Table 5.1). Identifying the other members of their gene families, or increasing the cDNA template concentration of *PcACS*, might unlock insights into their specific contributions to ethylene biosynthesis in response to biotic stress.

Table 5.1: Summary of target gene upregulation in response to *G. clavigera* and mountain pine beetle attack (MPB) relative to unwounded control. Black triangles indicate upregulation reflecting the same patterns as the hormone results. Red triangles indicate the different patterns from hormone results.

	Gene	Phloem				Xylem			
		G. clavigera		MPB		*G. clavigera*		MPB	
		7dpi	14dpi	1dpw	7dpw	7dpi	14dpi	1dpw	7dpw
JA Biosynthesis	*PcLOX*	▲			▲	▲	▲		▲
JA Biosynthesis	*PcAOS*								
JA Signaling	*PcJAZ*				▲				▲
ET Biosynthesis	*PcACO1*	▲	▲		▲	▲	▲		▲
	PcACO2	▲	▲		▲	▲	▲		▲
ET Biosynthesis	*PcACS*								

These findings can complement an ongoing transcriptome analysis of lodgepole pine responses to MPB attack versus *G. clavigera* inoculation using RNA-Seq, additionally, members of our lab are expanding our investigation to encompass more genes from the *PcJAZ* families. My research has revealed that the expression of certain JA and ET biosynthesis genes is triggered in response to MPB attack and inoculation with the fungus *G. clavigera*. However, the precise impact of *G. clavigera* on the tree's defense strategy against MPB attack is not yet fully clarified.

Some mature trees survive these MPB outbreaks, suggesting a natural selection process favoring beetle-resistant trees (Six et al. 2018, Cooke lab unpublished research). To further explain this aspect, our future research will compare the transcriptomic responses of MPB-resistant and susceptible lodgepole pine seedlings to *G. clavigera* inoculation. By doing so, we aim to decode the genetic underpinnings of tree survival and susceptibility. This investigation contributes to uncovering mechanisms that enable certain trees to withstand or succumb to MPB attacks, thereby advancing our comprehension of bark beetle-fungal interactions and plant defense mechanisms.

References

Abad, L. R., D'Urzo, M. P., Liu, D., Narasimhan, M. L., Reuveni, M., Zhu, J. K., Niu, X., Singh, N. K., Hasegawa, P. M., & Bressen, R. A. (1996). Antifungal activity of tobacco osmotin has specificity and involves plasma membrane permeabilization. *Plant Science 118*,11–23.

Arango-Velez, A., El Kayal, W., Copeland, C. C., Zaharia, L. I., Lusebrink, I., & Cooke, J. E. (2016). Differences in defence responses of Pinus contorta and Pinus banksiana to the mountain pine beetle fungal associate Grosmannia clavigera are affected by water deficit. *Plant, Cell and Environment*, *39*, 726–744.

Arango-Velez, A., González, L. M., Meents, M. J., El Kayal, W., Cooke, B. J., Linsky, J., Lusebrink, I., & Cooke, J. E. (2014) Influence of water deficit on the molecular responses of Pinus contorta x Pinus banksiana mature trees to infection by the mountain pine beetle fungal associate, Grosmannia clavigera. *Tree Physiology*, *34*, 1220–39.

Arnerup, J., Nemesio-Gorriz, M., Lundén, K., Asiegbu, F. O., Stenlid, J., & Elfstrand, M. (2013). The primary module in Norway spruce defence signalling against H. annosum s.l. seems to be jasmonate-mediated signalling without antagonism of salicylate-mediated signalling. *Planta*, *237*(4), 1037–1045

Azoulay, S. T., Schulze, S., Nissan, R. D., Bosmans, K., Shapira, O., Weckwerth, P., Zamora, O., Yarmolinsky, D., Trainin, T., Kollist, H., Huffaker, A., Rappel, W., & Schroeder, J. I. (2023). A role for ethylene signaling and biosynthesis in regulating and accelerating CO2- and abscisic acid-mediated stomatal movements in Arabidopsis. *New Phytologist*, *238*(6), 2460–2475.

Bale J. S. (2002). Insects and low temperatures: from molecular biology to distributions and abundance. *Philosophical Transactions of the Royal Society of London B: Biological Sciences 357*, 849-862.

Bentz B. J., & Mullins D. (1999) Ecology of mountain pine beetle (Coleoptera: Scolytidae) cold hardening in the intermountain west. *Environmental Entomology 28,* 577-587.

Bentz, B. J., Régnière, J., Fettig, C. J., Hansen, E. M., Hayes, J. L., Hicke, J. A., Kelsey, R. G., Negrón, J. F., & Seybold, S. J. (2010). Climate Change and Bark Beetles of the Western United States and Canada: Direct and Indirect Effects. *BioScience*, *60*(8), 602–613.

Bentz, B. J., & Six, D. L. (2006). Ergosterol content of fungi associated with *Dendroctonus ponderosae* and *Dendroctonus rufipennis* (Coleoptera: Curculionidae, Scolytinae). *Annals of the Entomological Society of America 99*, 189–194.

Bleiker, K. P., & Six, D. L. (2007). Dietary benefits of fungal associates to an eruptive herbivore: potential implications of multiple associates on host population dynamics. *Environmental* entomology, 36(6), 1384–1396.

Bleiker, K. P., Six, D. L., Potter, S. E., & Lauzon, C. R. (2009). Transport of fungal symbionts by mountain pine beetles. *Canadian Entomologist, 141*(5), 503-514–514.

Bleiker, K. P., & Uzunovic, A. (2004). Fast- and slow-growing subalpine fir produce lesions of different sizes in response to inoculation with a blue-stain fungus associated with Dryocoetes confusus (Coleoptera: Scolytidae). *Canadian Journal of Botany, 82*(6), 735–741.

Brush, M., & Lewis, M. A. (2023). Coupling Mountain Pine Beetle and Forest Population Dynamics Predicts Transient Outbreaks that are Likely to Increase in Number with Climate Change. *Bulletin of Mathematical Biology: A Journal Devoted to Research at the Interface of the Life and Mathematical Sciences*, *85*(11).

Bulens, I., de Poel, B. V., Hertog, M. L. A. T. M., De Proft, M. P., Geeraerd, A. H., & Nicolaï, B. M. (2011). Protocol: An updated integrated methodology for analysis of metabolites and enzyme activities of ethylene biosynthesis. *Plant Methods*, *7*(1), 17–26.

Burger, M., & Chory, J. (2019). Stressed Out About Hormones: How Plants Orchestrate Immunity. *CELL HOST & MICROBE*, *26*(2), 163–172.

Burns, I., Coltman, D. W., Cullingham, C. I., & James, P. M. A. (2019). Spatial and genetic structure of the lodgepole × jack pine hybrid zone. *Canadian Journal of Forest Research, 49*(7), 844-853–853.

Carlson, M. R., Berger, V. G., Murphy, J. C., & Ryrie, L. F. (2000). Genetics of elevational adaptations of lodgepole pine in the interior. *Journal of Sustainable Forestry*, *10*(1/2), 35.

Celedon, J. M., Bohlmann, J. (2019). Oleoresin defenses in conifers: chemical diversity, terpene synthases and limitations of oleoresin defense under climate change. *New Phytologist 224*:1444–1463.

Celedon, J. M., Yuen, M. M. S., Chiang, A., Henderson, H., Reid, K. E., & Bohlmann, J. (2017). Cell-type- and tissue-specific transcriptomes of the white spruce (Picea glauca) bark unmask

fine-scale spatial patterns of constitutive and induced conifer defense. *Plant Journal*, *92*(4), 710-726–726.

Chiu, C. C., Keeling, C. I., & Bohlmann, J. (2017). Toxicity of Pine Monoterpenes to Mountain Pine Beetle. *Scientific Reports*, *7*(1), 1–8.

Chiu, C. C., & Bohlmann, J. (2022). Mountain Pine Beetle Epidemic: An Interplay of Terpenoids in Host Defense and Insect Pheromones. *Annual Review Plant Biology*, *73*, 475–494.

Cook, S. P., Shirley, B. M., &Zambino, P. J. (2010). Nitrogen concentration in mountain pine beetle larvae reflects nitrogen status of the tree host and two fungal associates. *Environmental Entomology 39,* 821–826.

Creelman, R. A., & Mullet, J. E. (1997). Biosynthesis and Action of Jasmonates in Plants. *Annual Review of Plant Physiology & Plant Molecular Biology, 48*(1), 355.

Critchfield, W. B. (1985). The late Quaternary history of lodgepole and jack pines. *Canadian Journal of Forest Research*, *15*(5), 749-772–772.

Cudmore, T. J., Björklund, N., Carroll, A. L., & Lindgren, B. S. (2010). Climate change and range expansion of an aggressive bark beetle: evidence of higher beetle reproduction in naïve host tree populations. *Journal of Applied Ecology, 47*(5), 1036–1043.

Cui, H., Tsuda, K., & Parker, J. E. (2015). Effector-triggered immunity: from pathogen perception to robust defense. *Annual Review of Plant Biology 66***,** 487-511.

Cullingham, C. I., Cooke, J. E., Dang, S., Davis, C. S., Cooke, B. J., & Coltman, D. W. (2011). Mountain pine beetle host-range expansion threatens the boreal forest. *Molecular ecology*, *20*(10), 2157–2171.

Dangl, J. L., Horvath, D. M., & Staskawicz, B. J. (2013). Pivoting the plant immune system from dissection to deployment. *Science 341*, 746-751.

Deslandes, L., & Rivas, S. (2012). Catch me if you can: bacterial effectors and plant targets. *Trends in Plant Science 17*, 644-655.

Dhar, A., Parrott, L., & Heckbert, S. (2016). Consequences of mountain pine beetle outbreak on forest ecosystem services in western Canada. *Canadian Journal of Forest Research*, *46*(8), 987–999.

DiGuistini, S., Wang, Y., Liao, N. Y., Taylor, G., Tanguay, P., Feau, N., Henrissat, B., Chan, S. K., Hesse-Orce, U., Alamouti, S. M., Tsui, C. K., Docking, R. T., Levasseur, A., Haridas, S., Robertson, G., Birol, I., Holt, R. A., Marra, M. A., Hamelin, R. C., Hirst, M., … Breuil, C. (2011). Genome and transcriptome analyses of the mountain pine beetle-fungal symbiont Grosmannia clavigera, a lodgepole pine pathogen. *Proceedings of the National Academy of Sciences of the United States of America, 108*(6), 2504–2509.

Erb, M., & Reymond, P. (2019). Molecular interactions between plant and herbivores. *Annu. Rev. Plant Biol. 70*, 527–57

Erbilgin, N., Ma, C., Shan, B., Najar, A., Whitehouse, C., & Evenden, M. (2014). Chemical similarity between historical and novel host plants promotes range and host expansion of the mountain pine beetle in a naïve host ecosystem. *New Phytologist*, *201*(3), 940-950–950.

Eyles A., Bonello P., Ganley E. & Mohammed C. (2010) Induced resistance to pests and pathogens in trees. *New Phytologist 185***,** 893–908

Fett-Neto, A.G., Rodrigues-Corrêa, K.C.S. (2012). Physiological control of pine resin production. In: Fett-Neto, A.G., Rodrigues-Corrêa, K.C.S. (Eds.), *Pine Resin: Biology*

Ferrenberg, S., Kane, J. M., & Mitton, J. B. (2014). Resin duct characteristics associated with tree resistance to bark beetles across lodgepole and limber pines. *Oecologia*, *174*(4), 1283–1292

Franceschi, V. R., Krekling, T., Berryman, A. A., & Christiansen, E. (1998). Specialized Phloem Parenchyma Cells in Norway Spruce (Pinaceae) Bark are an Important Site of Defense Reactions. *American Journal of Botany*, *85*(5), 601–615.

Fortier, C. E. (2022). *Conifer Chemical and Structural Defenses Against Pests and Pathogens* [University of Alberta. Department of Biological Sciences.].

Fortier, C. E., Musso, A. E., Evenden, M. L., Zaharia, L. I., & Cooke, J. (2024). Evidence that ophiostomatoid fungal symbionts of mountain pine beetle do not play a role in overcoming lodgepole pine defenses during mass attack. *Molecular Plant-Microbe Interactions.*

Franceschi, V. R., Krokene, P., Christiansen, E., & Krekling, T. (2005). Anatomical and chemical defenses of conifer bark against bark beetles and other pests. *The New phytologist*, *167*(2), 353–375.

Franceschi, V. R., Krokene, P., & Christiansen, E. (2002). Application of methyl jasmonate on Picea abies (Pinaceae) stems induces defense-related responses in phloem and xylem. *Am. J. Bot. 89*, 578–586.

Gaylord, M. L., Kolb, T. E., and McDowell, N. G. (2015). Mechanisms of Piñon pine mortality after severe drought: a retrospective study of mature trees. *Tree Physiol. 35*, 806–816.

Glazebrook, J. (2005). Contrasting Mechanisms of Defense against Biotrophic and Necrotrophic Pathogens. *Annual Review of Phytopathology, 43*(1), 205–227.

Goodsman, D. W., Erbilgin, N., & Lieffers, V. J. (2012). The impact of phloem nutrients on overwintering mountain pine beetles and their fungal symbionts. *Environmental entomology*, *41*(3), 478–486.

Heyman, J., Canher, B., Bisht, A., Christiaens, F., & D Veylder, L. (2018). Emerging role of the plant ERF transcription factors in coordinating wound defense responses and repair. *Journal of Cell Science: 131*, jcs208215

Hood, S. M., and Sala, A. (2015). Ponderosa pine resin defenses and growth: metrics matter. *Tree Physiol. 35*, 1223–1235.

Hothorn, T., Bretz, F., & Westfall, P. (2008). Simultaneous inference in general parametric models. *Biometrical Journal, 50*(3), 346-363.

Huber, D. P. W., Ralph, S., & Bohlmann, J. (2004). Genomic Hardwiring and Phenotypic Plasticity of Terpenoid-Based Defenses in Conifers. *Journal of Chemical Ecology*, *30*(12), 2399–2418.

Hudgins, J. W., Christiansen, E., & Franceschi, V. (2004). Induction of anatomically based defense responses in stems of diverse conifers by methyl jasmonate: a phylogenetic perspective. *Tree Physiology, 24*(3), 251–264.

Hudgins, J. W., Krekling, T., & Franceschi, V. R. (2003). Distribution of Calcium Oxalate Crystals in the Secondary Phloem of Conifers: A Constitutive Defense Mechanism? *The New Phytologist*, *159*(3), 677–690

Hudgins, J. W., Ralph, S. G., Franceschi, V. R., & Bohlmann, J. (2006). Ethylene in induced conifer defense: cDNA cloning, protein expression, and cellular and subcellular localization of 1-aminocyclopropane-1-carboxylate oxidase in resin duct and phenolic parenchyma cells. *Planta, 224*(4), 865–877.

Hyong Woo Choi, & Klessig, D. F. (2016). DAMPs, MAMPs, and NAMPs in plant innate immunity. *BMC Plant Biology, 16*, 1–10.

James, P. M. A., & Huber, D. P. W. (2019). TRIA-Net: 10 years of collaborative research on turning risk into action for the mountain pine beetle epidemic. *Canadian Journal of Forest Research*, *49*(12), III–V.

Jones, J. D., & Dangl, J. L. (2006). The plant immune system. *Nature 444***,** 323-3

Kane, J. M., & Kolb, T. E. (2010). Importance of resin ducts in reducing ponderosa pine mortality from bark beetle attack. *Oecologia*, *164*(3), 601–609.

Karasov, T. L., Horton, M. W., & Bergelson, J. (2014). Genomic variability as a driver of plant–pathogen coevolution? *Current Opinion in Plant Biology 18***,** 24-30.

Katoh, K., Rozewicki, J., & Yamada, K. D. (2019). MAFFT online service: multiple sequence alignment, interactive sequence choice and visualization. *Briefings in Bioinformatics*, 1160–1166.

Kayal, W. E., Cooke, B. J., Linsky, J., Arango-Velez, A., Galindo González, L. M., Cooke, J. E. K., Meents, M. J., & Lusebrink, I. (2013). *Influence of water deficit on the molecular responses of Pinus contorta × Pinus banksiana mature trees to infection by the mountain pine beetle fungal associate, Grosmannia clavigera.*

Keeling C. I. & Bohlmann J. (2006) Diterpene resin acids in conifers. *Phytochemistry **67***, 2415-2423.

Khadempour, L., LeMay, V., Jack, D., Bohlmann, J., & Breuil, C. (2012). The Relative Abundance of Mountain Pine Beetle Fungal Associates Through the Beetle Life Cycle in Pine Trees. *Microbial Ecology*, *64*(4), 909–917.

Kim, J.-J., Plattner, A., Lim, Y. W., & Breuil, C. (2008). Comparison of two methods to assess the virulence of the mountain pine beetle associate, Grosmannia clavigera, to Pinus contorta. *Scandinavian Journal of Forest Research*, *23*(2), 98–104.

Klepzig, K. D., & Six, D. L. (2004) Bark beetle-fungal symbiosis: context dependency in complex associations. *Symbiosis 37*, 189–205.

Klutsch, J., Najar, A., Sherwood, P., Bonello, P., & Erbilgin, N. (2017). A Native Parasitic Plant Systemically Induces Resistance in Jack Pine to a Fungal Symbiont of Invasive Mountain Pine Beetle. *Journal of Chemical Ecology, 43*(5), 506–518.

Kopaczyk, J. M., Warguła, J., Jelonek, T. (2020) The variability of terpenes in conifers under developmental and environmental stimuli. *Environmental and Experimental Botany 180,* 104197.

Lacerda, A. F., Vasconcelos, E. A. R., Pelegrini, P. B., & Grossi de Sa, M. F. (2014). Antifungal defensins and their role in plant defense. *Frontiers in Microbiology*, *5*(APR).

Lee, S., Breuil, C., & Kim, J.-J. (2006). Diversity of fungi associated with the mountain pine beetle, Dendroctonus ponderosae and infested lodgepole pines in British Columbia. *Fungal Diversity, 22*, 91-105–105.

Lenth, R. (2020). *emmeans: Estimated marginal means, aka least-squares means* [R package version 1.5.3]. CRAN R Project. https://CRAN.R-project.org/package=emmeans

Levene, H. (1960). Robust tests for equality of variances. In I. Olkin, S. G. Ghurye, W. Hoeffding, & W. G. Madow (Eds.), *Contributions to Probability and Statistics: Essays in Honor of Harold Hotelling* (pp. 278–292). Stanford University Press.

Li, H., & Ecker, J. R. (2002). Ethylene Biosynthesis and Signaling Networks. *The Plant Cell, 14*, S131–S151.

Li, S. -H., Hammerbacher, A., Niu, X.-M., Gershenzon, J., Schneider, B., Nagy, N. E., & Krokene, P. (2012). Localization of Phenolics in Phloem Parenchyma Cells of Norway Spruce (Picea abies). *ChemBioChem*, *13*(18), 2707-2713–2713.

Liu, J. -J., Sturrock, R., Ekramoddoullah, A. K. M. (2010). The superfamily of thaumatin-like proteins: its origin, evolution, and expression towards biological function. *Plant Cell Reports 29*, 419–436.

Lusebrink, I., Erbilgin, N., & Evenden, M. L. (2013). The lodgepole × jack pine hybrid zone in Alberta, Canada: a stepping stone for the mountain pine beetle on its journey East across the boreal forest? *Journal of chemical ecology*, *39*(9), 1209–1220.

Lieutier, F., Salle, A., & Yart, A. (2009). Stimulation of tree defenses by Ophiostomatoid fungi can explain attack success of bark beetles on conifers. *Annals of Forest Science, 66*(8), 801-801–801.

Liu, M., Jaber, E., Zeng, Z., Kovalchuk, A., Asiegbu, F. O. (2021) Physiochemical and molecular features of the necrotic lesion in the *Heterobasidion* –Norway spruce pathosystem Mock H-P (ed). *Tree Physiology 41*:791–800.

Mahon, E. L. (2016). *Molecular analysis of lodgepole and jack pine seedlings response to inoculation by mountain pine beetle fungal associate Grosmannia clavigera under well watered and water deficit* [University of Alberta. Department of Biological Sciences.].

Martin, D., Tholl, D., Gershenzon, J., & Bohlmann, J. (2002). Methyl Jasmonate Induces Traumatic Resin Ducts, Terpenoid Resin Biosynthesis, and Terpenoid Accumulation in Developing Xylem of Norway Spruce Stems. *Plant Physiology*, *129*(3), 1003–1018.

McAllister, C. H., Fortier, C. E., St Onge, K. R., Sacchi, B. M., Nawrot, M. J., Locke, T., & Cooke, J. E. K. (2018). A novel application of RNase H2-dependent quantitative PCR for detection and quantification of Grosmannia clavigera, a mountain pine beetle fungal symbiont, in environmental samples. *Tree Physiology, 38*(3), 485-501–501.

Nagy, N. E., Franceschi, V. R., Solheim, H., Krekling, T., & Christiansen, E. (2000). Wound-Induced Traumatic Resin Duct Development in Stems of Norway Spruce (Pinaceae): Anatomy and Cytochemical Traits. *American Journal of Botany, 87*(3), 302–313.

Nagy, N. E., Krokene, P., Hietala, A. M., Solheim, H., Fossdal, C. G., & Sikora, K. (2014). Using laser micro-dissection and qRT-PCR to analyze cell type-specific gene expression in Norway spruce phloem. *PeerJ*, *2014*(1).

Nagy, N. E., Kvaalen, H., Fongen, M., Fossdal, C. G., Clarke, N., Solheim, H., & Hietala, A. M. (2012). The pathogenic white-rot fungus Heterobasidion parviporum responds to spruce xylem defense by enhanced production of oxalic acid. *Molecular Plant-Microbe Interactions*, *25*(11), 1450-1458–1458.

Nagy, N. E., Norli, H. R., Fongen, M., Østby, R. B., Heldal, I. M., Davik, J., & Hietala, A. M. (2022). Patterns and roles of lignan and terpenoid accumulation in the reaction zone compartmentalizing pathogen-infected heartwood of Norway spruce. *Planta: An International Journal of Plant Biology*, *255*(3), 1–14.

Natural Resource Canada, Canadian Forest service (2015). *Lodgepole pine.* Trees, insects and diseases of Canada's forests. https://tidcf.nrcan.gc.ca/en/trees/factsheet/140

Neuhaus, J. -M. (1999). Plant chitinases (PR-3, PR-4, PR-8, PR-11). In: S. K. Datta, S. Muthukrishnan (eds) *Pathogenesis-Related Proteins in Plants, 1st edn*.p 29.

Ngou, B. P. M., Ahn, H.-K., Ding, P., & Jones, J. D. G. (2021). Mutual potentiation of plant immunity by cell-surface and intracellular receptors. *Nature: International Weekly Journal of Science*, *592*(7852), 110–115.

Paine, T. D., Raffa, K. F., & Harrington, T. C. (1997). Interactions among Scolytid bark beetles, their associated fungi, and live host conifers. *Annual review of entomology*, *42*, 179–206.

Pan, Y., Zhao, T., Krokene, P., Yu, Z., Qiao, M., Lu, J., Chen, P., Ye, H. (2018). Bark beetle-associated blue-stain fungi increase antioxidant enzyme activities and monoterpene concentrations in Pinus yunnanensis. *Frontiers in Plant Science 9*, 1731.

Pavy, N., Boyle, B., Nelson, C., Paule, C., Giguère, I., Caron, S., Parsons, L. S., Dallaire, N., Bedon, F., Bérubé, H., Cooke, J., & Mackay, J. (2008). Identification of conserved core xylem gene sets: conifer cDNA microarray development, transcript profiling and computational analyses. *The New phytologist*, *180*(4), 766–786.

Peery, R. M., McAllister, C. H., Cullingham, C. I., Mahon, E. L., Arango-Velez, A., & Cooke, J. E. K. (2021). *Comparative genomics of the chitinase gene family in lodgepole and jack pines: contrasting responses to biotic threats and landscape level investigation of genetic differentiation*.

Pieterse, C. M., Leon-Reyes, A., Van der Ent, S., & Van Wees, S. C. (2009). Networking by small-molecule hormones in plant immunity. *Nature chemical biology*, *5*(5), 308–316.

Plattner A., Kim J., Diguistini S., & Breuil, C. (2008) Variation in pathogenicity of a mountain pine beetle – associated blue-stain fungus, Grosmannia clavigera, on young lodgepole pine in British Columbia. *Forest Pathology*, *466*, 457–466.

Pureswaran, D.S., Gries, R., & Borden, J.H. (2004) Quantitative variation in monoterpenes in four species of conifers. *Biochemical Systematics and Ecology 32*, 1109–1136.

Raffa, K. F. (1983). Physiological Aspects of Lodgepole Pine Wound Responses to a Fungal Symbiont of the Mountain Pine Beetle, Dendroctonus Ponderosae (Coleoptera: Scolytidae). *The Canadian Entomologist, 115*(7), 723-734–734.

Raffa, K. F. (2014). Terpenes Tell Different Tales at Different Scales: Glimpses into the Chemical Ecology of Conifer - Bark Beetle - Microbial Interactions. *Journal of Chemical Ecology*, *40*(1), 1-20–20.

Raffa, K. F., Aukema, B. H., Bentz, B. J., Carroll, A. L., Hicke, J. A., Turner, M. G., & Romme, W. H. (2008). Cross-scale Drivers of Natural Disturbances Prone to Anthropogenic Amplification: The Dynamics of Bark Beetle Eruptions. *BioScience, 58*(6), 501–517.

Raffa, K. F., & Berryman, A. A. (1983). The role of host plant resistance in the colonization behavior and ecology of bark beetles (Coleoptera: Scolytidae). *Ecological Monographs 53*, 27–49.

Raffa, K. F., & Smalley, E. B. (1995). Interaction of pre-attack and induced monoterpene concentrations in host conifer defense against bark beetle-fungal complexes. *Oecologia*, *102*(3), 285–295.

Raffa, K. F., Grégoire, J.-C., & Lindgren, B. S. (2015). Natural history and ecology of bark beetles. In F. E. Vega & R. W. Hofstetter (Eds.), *Bark Beetles: Biology and Ecology of Native and Invasive Species* (pp. 1–40). Academic Press, Elsevier.

Raffa, K. F., Powell, E. N., & Townsend, P. A. (2013) Temperature-driven range expansion of an irruptive insect heightened by weakly coevolved plant defenses. *Proceedings of the National Academy of Sciences USA* ***110***, 2193-2198.

Raffaele, S., Farrer, R. A., Cano, L. M., Studholme, D. J., MacLean, D., Thines, M. & Meyers, B. C. (2010). Genome evolution following host jumps in the Irish potato famine pathogen lineage. *Science 330*, 1540-1543.

Richard, S., Séguin, A., Lapointe, G., & Rutledge, R. G. (2000). Induction of chalcone synthase expression in white spruce by wounding and jasmonate. *Plant and Cell Physiology, 41*(8), 982-987–987.

Richardson, D. M. (2000). *Ecology and biogeography of Pinus*. Cambridge University Press.

Rodrigues-Corrêa, K.C.S., Lima, J.C., & Fett-Neto, A.G. (2012). Pine oleoresin: tapping green chemicals, biofuels, food protection, and carbon sequestration from multipurpose trees. *Food Energy Secur. 1*, 81–93.

Roe, A. D., James, P. M., Rice, A. V., Cooke, J. E., & Sperling, F. A. (2011). Spatial community structure of mountain pine beetle fungal symbionts across a latitudinal gradient. *Microbial ecology*, *62*(2), 347–360.

Rweyongeza, D. M., Barnhardt, L. K., & Hansen, C. R. (2010). *Patterns of optimal growth for lodgepole pine provenances in Alberta*. Alberta Sustainable Resource Development, Alberta Tree Improvement & Seed Centre.

Safranyik L., Carroll A. L. (2006) The biology and epidemiology of the mountain pine beetle in lodgepole pine forests. In: *The Mountain Pine Beetle: A Synthesis of Biology, Management and Impacts on Lodgepole Pine.* Natural Resources Canada, Canadian Forest Service, Pacific Forestry Centre, Victoria, British Columbia, pp 3–66.

Safranyik, L., Carroll, A. L., Regniere, J., Langor, D. W., Riel, W. G., Shore, T. L., Peter, B., Cooke, B. J., Nealis, V. G., & Taylor, S. W. (2010). Potential for range expansion of mountain pine beetle into the boreal forest of North America. *Canadian Entomologist*, *142* (5), 415–442.

Shapiro, S. S., & Wilk, M. B. (1965) An analysis of variance test for normality (complete samples). *Biometrika 52*, 591–611.

Six, D. L. (2020). A major symbiont shift supports a major niche shift in a clade of tree-killing bark beetles. *Ecological Entomology, 45*(2), 190-201–201.

Six, D. L., Bentz, B. J. (2007). Temperature determines the relative abundance of symbionts in a multipartite bark beetle-fungus symbiosis. *Microb. Ecol. 54*, 112–18

Six, D. L., Harrington, T. C., Steimel, J., McNew, D., & Paine, T. D. (2003). Genetic relationships among Leptographium terebrantis and the mycangial fungi of three western *Dendroctonus* bark beetles. *Mycologia*, *95*(5), 781–792.

Six, D. L., & Klepzig, K. D. (2004). Dendroctonus bark beetles as model systems for studies on symbiosis. *Symbiosis **37*,** 207-232.

Six, D. L., & Klepzig, K. D. (2021). Context dependency in bark beetle-fungus mutualisms revisited: assessing potential shifts in interaction outcomes against varied genetic, ecological, and evolutionary backgrounds. *Frontiers in Microbiology 12*, 682187.

Six, D. L., & Paine, T. D. (1998). Effects of Mycangial Fungi and Host Tree Species on Progeny Survival and Emergence of Dendroctonus ponderosae (Coleoptera: Scolytidae). *Environmental Entomology, 27*(6), 1393-1401–1401.

Six, D. L., Vergobbi, C., & Cutter, M. (2018). Are survivors different? Genetic-based selection of trees by mountain pine beetle during a climate change-driven outbreak in a high-elevation pine forest. *Frontiers in Plant Science, 9*.

Six, D. L., & Wingfield, M. J. (2011). The role of phytopathogenicity in bark beetle-fungus symbioses: a challenge to the classic paradigm. *Annual review of entomology*, *56*, 255–272.

Soderberg, D. N., Kyre, B., Bonello, P., & Bentz, B. J. (2021). Lignin concentrations in phloem and outer bark are not associated with resistance to mountain pine beetle among high elevation pines. *PLoS ONE, 16*(9), 1–12.

Solheim, H., & Krokene, P. (1998). Growth and virulence of mountain pine beetle associated blue-stain fungi, Ophiostoma clavigerum and Ophiostoma montium. *Canadian Journal of Botany*, *566*, 561–566.

Spatafora, J. W., & Blackwell, M. (1994). The polyphyletic origins of ophiostomatoid fungi. *Mycol. Res. 98*, 1–9

Van Loon, L.C., Rep, M. & Pieterse, C. M. J., (2006) Significance of inducible defense-related proteins in infected plants. *Annual Review of Phytopathology 44*,135–162

Vazquez-Gonzalez, C., Sampedro, L., Lopez-Goldar, X., Solla, A., Vivas, M., Rozas, V., Josefa Lombardero, M., & Zas, R. (2022). Inducibility of chemical defences by exogenous application of methyl jasmonate is long-lasting and conserved among populations in mature Pinus pinaster trees. *FOREST ECOLOGY AND MANAGEMENT*, *518*, 120280.

Vázquez-González, C., Zas, R., Erbilgin, N., Ferrenberg, S., Rozas, V., & Sampedro, L. (2020). Resin ducts as resistance traits in conifers: linking dendrochronology and resin-based defences. *Tree Physiology*, *40*(10), 1313–1326.

Wasternack, C., & Song, S. (2017). Jasmonates : biosynthesis, metabolism, and signaling by proteins activating and repressing transcription. *Journal of Experimental Botany, 68*(6), 1303–1321.

Whitehill, J. G. A., Yuen, M. M. S., Henderson, H., Madilao, L., Kshatriya, K., Bryan, J., Jaquish, B., & Bohlmann, J. (2019). Functions of stone cells and oleoresin terpenes in the conifer defense syndrome. *The New Phytologist*, *221*(3), 1503–1517.

Wickham, H. (2016). *ggplot2: Elegant graphics for data analysis.* Springer-Verlag. https://ggplot2.tidyverse.org

Wilke, C. O. (2020). *cowplot: Streamlined plot theme and plot annotations for* 'ggplot2' [R package version 1.1.1]. CRAN R Project. https://CRAN.R-project.org/package=cowplot

Wingfield, M. J. (1986). Pathogenicity of Leptographium procerum and L. terebrantis on Pinus strobus seedlings and established trees. *Eur. J. For. Pathol. 16*, 299–308

Witzell, J., & Martín, J. A. (2008). Phenolic metabolites in the resistance of northern forest trees to pathogens — past experiences and future prospects. *Canadian Journal of Forest Research*, *38*(11), 2711–2727.

Wood, D. L. (1982). The role of pheromones, kairomones, and allomones in the host selection and colonization behavior of bark beetles. *Annual Review of Entomology*, *27*(1), 411–446.

Yoshida, H., Nagata, M., Saito, K., Wang, K. & Ecker, J. (2005). Arabidopsis ETO1 specifically interacts with and negatively regulates type 2 1-aminocyclopropane-1-carboxylate synthases. *BMC Plant Biol. 5*, 14.

Yuan, M., Jiang, Z., Bi, G., Nomura, K., Liu, M., Wang, Y., Cai, B., Zhou, J. -M., He, S. Y., Xin, X. -F (2021). Pattern-recognition receptors are required for NLR-mediated plant immunity. *Nature: International Weekly Journal of Science*, *592*(7852),

Zaman, R., May, C., Ullah, A., & Erbilgin, N. (2023). Bark Beetles Utilize Ophiostomatoid Fungi to Circumvent Host Tree Defenses. *Metabolites, 13*(2).

Zeneli, G., Gershenzon, J., Krokene, P., Christiansen, E., & Krekling, T. (2006). Methyl jasmonate treatment of mature Norway spruce (Picea abies) trees increases the accumulation of terpenoid resin components and protects against infection by Ceratocystis polonica, a bark beetle-associated fungus. *Tree Physiology*, *26*(8), 977-988–988.

Zhao, S., and Erbilgin, N. (2019). Larger resin ducts are linked to the survival of lodgepole pine trees during mountain pine beetle outbreak. *Front. Plant Sci.* 10:1459.

Zipfel, C. (2014). Plant pattern-recognition receptors. *Trends in Immunology, 35*(7), 345–351.

Appendix 1

List of Tables

Table 1. Summary of analysis of deviance of generalized linear mixed models fit to phloem JA & ET biosynthesis and JA signaling qRT-PCR expression data. Asterisks (*) indicate interactions between factors. All genes were fit to the following formula: transcript abundance ~ time point * treatment, family = Gamma (link = log).

	***G. clavigera* inoculation**			**MPB attack**		
	df	**χ^2**	***p***	**df**	**χ^2**	***p***
PcLipoxygenase (PcLOX)						
Treatment	2	14.91	$\mathbf{5.78 \times 10^{-4}}$	2	13.32	$\mathbf{1.28 \times 10^{-3}}$
Timepoint	1	1.03	3.09×10^{-1}	1	12.77	$\mathbf{3.53 \times 10^{-4}}$
Treatment * Timepoint	2	5.51	6.36×10^{-2}	2	12.34	$\mathbf{2.09 \times 10^{-3}}$
PcAllene Oxide Synthase (PcAOS)						
Treatment	2	4.25	1.20×10^{-1}	2	3.37	1.86×10^{-1}
Timepoint	1	0.55	4.58×10^{-1}	1	0.02	8.92×10^{-1}
Treatment * Timepoint	2	0.04	9.80×10^{-1}	2	1.97	3.74×10^{-1}
PcJasmonate-Zim Domain Protein (PcJAZ)						
Treatment	2	1.41	4.95×10^{-1}	2	5.99	5.01×10^{-2}
Timepoint	1	0.37	5.42×10^{-1}	1	3.56	5.91×10^{-2}
Treatment * Timepoint	2	2.35	3.10×10^{-1}	2	10.7	$\mathbf{4.74 \times 10^{-3}}$
Pc1-Aminocyclopropane-1-Carboxylic Acid synthase (PcACS)						
Treatment	2	42.47	$\mathbf{5.99 \times 10^{-10}}$	2	0.44	8.02×10^{-1}
Timepoint	1	1.73	1.88×10^{-1}	1	3.06	8.02×10^{-2}
Treatment * Timepoint	2	3.31	1.91×10^{-1}	2	17.09	$\mathbf{1.94 \times 10^{-4}}$
Pc1-Aminocyclopropane-1-Carboxylic Acid Oxidases 1 (PcACO1)						
Treatment	2	119.22	$\mathbf{1.29 \times 10^{-26}}$	2	14.34	$\mathbf{7.69 \times 10^{-4}}$
Timepoint	1	0.69	4.07×10^{-1}	1	2.95	8.59×10^{-2}
Treatment * Timepoint	2	3.51	1.73×10^{-1}	2	29.95	$\mathbf{3.14 \times 10^{-7}}$
Pc1-Aminocyclopropane-1-Carboxylic Acid Oxidases 2 (PcACO2)						
Treatment	2	69.27	$\mathbf{9.06 \times 10^{-16}}$	2	4.75	9.29×10^{-2}
Timepoint	1	19.76	$\mathbf{8.78 \times 10^{-6}}$	1	0.15	6.97×10^{-1}
Treatment * Timepoint	2	0.13	9.36×10^{-1}	2	7.39	$\mathbf{2.49 \times 10^{-2}}$

Table 2. Summary of analysis of deviance of generalized linear mixed models fit to xylem JA & ET biosynthesis and JA signaling qRT-PCR expression data. Asterisks (*) indicate interactions between factors. All genes were fit to the following formula: transcript abundance ~ time point * treatment, family = Gamma (link = log).

	***G. clavigera* inoculation**			**MPB attack**		
	df	**χ^2**	***p***	**df**	**χ^2**	***p***
PcLipoxygenase (PcLOX)						
Treatment	2	24.3	$\mathbf{5.28 \times 10^{-6}}$	2	21.08	$\mathbf{2.65 \times 10^{-5}}$
Timepoint	1	1.13	2.87×10^{-1}	1	21.36	$\mathbf{3.80 \times 10^{-6}}$
Treatment * Timepoint	2	2.73	2.55×10^{-1}	2	15.24	$\mathbf{4.91 \times 10^{-4}}$
PcAllene Oxide Synthase (PcAOS)						
Treatment	2	0.95	6.23×10^{-1}	2	1.02	5.99×10^{-1}
Timepoint	1	3.02	8.20×10^{-2}	1	0.32	5.74×10^{-1}
Treatment * Timepoint	2	0.05	9.77×10^{-1}	2	2.85	2.40×10^{-1}
PcJasmonate-Zim Domain Protein (PcJAZ)						
Treatment	2	7.65	$\mathbf{2.18 \times 10^{-2}}$	2	22.8	$\mathbf{1.12 \times 10^{-5}}$
Timepoint	1	2.08	1.50×10^{-1}	1	0.51	4.74×10^{-1}
Treatment * Timepoint	2	1.79	4.09×10^{-1}	2	24.17	$\mathbf{5.63 \times 10^{-6}}$
Pc1-Aminocyclopropane-1-Carboxylic Acid synthase (PcACS)						
Treatment	2	30.2	$\mathbf{2.77 \times 10^{-7}}$	2	63.45	$\mathbf{1.67 \times 10^{-14}}$
Timepoint	1	0.85	3.57×10^{-1}	1	43.04	$\mathbf{5.37 \times 10^{-11}}$
Treatment * Timepoint	2	5.81	5.47×10^{-2}	2	19.67	$\mathbf{5.35 \times 10^{-5}}$
Pc1-Aminocyclopropane-1-Carboxylic Acid Oxidases 1 (PcACO1)						
Treatment	2	158.12	$\mathbf{4.62 \times 10^{-35}}$	2	25.54	$\mathbf{2.85 \times 10^{-6}}$
Timepoint	1	4.41	$\mathbf{3.57 \times 10^{-2}}$	1	6.03	$\mathbf{1.41 \times 10^{-2}}$
Treatment * Timepoint	2	17.26	$\mathbf{1.79 \times 10^{-4}}$	2	74.12	$\mathbf{8.02 \times 10^{-17}}$
Pc1-Aminocyclopropane-1-Carboxylic Acid Oxidases 2 (PcACO2)						
Treatment	2	64.76	$\mathbf{8.67 \times 10^{-15}}$	2	37.16	$\mathbf{8.54 \times 10^{-9}}$
Timepoint	1	23.74	$\mathbf{1.11 \times 10^{-6}}$	1	0.2	6.57×10^{-1}
Treatment * Timepoint	2	2.25	3.24×10^{-1}	2	16.42	$\mathbf{2.72 \times 10^{-4}}$

Table 3. Summary of analysis of deviance of generalized linear mixed models fit to phloem reference gene qRT-PCR expression data. Asterisks (*) indicate interactions between factors. All genes were fit to the following formula: transcript abundance ~ time point * treatment, family = Gamma (link = log). The arithmetic mean of *PcUBA1* and *PcVHA-A* exhibits a significant difference across various treatments and timepoints (p = 0), leading to the decision against using a single reference gene or a combination of two reference genes; instead, the arithmetic mean of *PcUBC11*, *PcVHA-A*, and *PcUBA1* was employed for data normalization.

	***G. clavigera* inoculation**			**MPB attack**		
	df	**χ^2**	***p***	**df**	**χ^2**	***p***
PcUbiquitin-activating enzyme 1 (PcUBA1)						
Treatment	2	0	9.98×10^{-1}	2	0.41	8.15×10^{-1}
Timepoint	1	0.39	5.33×10^{-1}	1	0.26	6.11×10^{-1}
Treatment * Timepoint	2	1.12	5.73×10^{-1}	2	0.46	7.93×10^{-1}
PcUbiquitin-conjugating enzyme 11 (PcUBC11)						
Treatment	2	0.53	7.67×10^{-1}	2	0.26	8.77×10^{-1}
Timepoint	1	0.63	4.29×10^{-1}	1	0.15	7.03×10^{-1}
Treatment * Timepoint	2	1.33	5.14×10^{-1}	2	1.89	3.89×10^{-1}
PcVacuolar ATP synthase subunit A (PcVHA-A)						
Treatment	2	0.08	9.60×10^{-1}	2	0.47	7.92×10^{-1}
Timepoint	1	0.16	6.91×10^{-1}	1	0.02	8.86×10^{-1}
Treatment * Timepoint	2	1.21	5.47×10^{-1}	2	1.8	4.07×10^{-1}
Arithmetic Mean of PcUBA1 and PcVHA-A						
Treatment	2	0.05	9.75×10^{-1}	2	9,833.49	**0**
Timepoint	1	0.22	6.36×10^{-1}	1	2,723.18	**0**
Treatment * Timepoint	2	1.06	5.89×10^{-1}	2	16,673.05	**0**
Arithmetic Mean of PcUBA1 and PcUBC11						
Treatment	2	0.31	8.57×10^{-1}	2	0.26	8.80×10^{-1}
Timepoint	1	0.58	4.47×10^{-1}	1	0.02	8.82×10^{-1}
Treatment * Timepoint	2	1.31	5.20×10^{-1}	2	1.45	4.84×10^{-1}
Arithmetic Mean of PcUBC11 and PcVHA-A						
Treatment	2	0.11	9.44×10^{-1}	2	0.34	8.44×10^{-1}

Timepoint	1	0.4	5.27×10^{-1}	1	0.08	7.80×10^{-1}
Treatment * Timepoint	2	1.31	5.20×10^{-1}	2	1.73	4.21×10^{-1}
Geometric Mean of PcUBA1 and PcVHA-A						
Treatment	2	0.03	9.85×10^{-1}	2	8,478.96	**0**
Timepoint	1	0.27	6.03×10^{-1}	1	2,139.15	**0**
Treatment * Timepoint	2	1.02	5.99×10^{-1}	2	15,135.55	**0**
Geometric Mean of PcUBA1 and PcUBC11						
Treatment	2	0.1	9.53×10^{-1}	2	0.29	8.65×10^{-1}
Timepoint	1	0.49	4.85×10^{-1}	1	0.01	9.07×10^{-1}
Treatment * Timepoint	2	1.2	5.48×10^{-1}	2	0.97	6.16×10^{-1}
Geometric Mean of PcUBC11 and PcVHA-A						
Treatment	2	0.05	9.76×10^{-1}	2	0.35	8.38×10^{-1}
Timepoint	1	0.34	5.61×10^{-1}	1	0.08	7.82×10^{-1}
Treatment * Timepoint	2	1.34	5.12×10^{-1}	2	1.8	4.06×10^{-1}
Arithmetic Mean of PcUBC11, PcVHA-A, and PcUBA1						
Treatment	2	0.08	9.61×10^{-1}	2	0.33	8.48×10^{-1}
Timepoint	1	0.4	5.25×10^{-1}	1	0.02	8.86×10^{-1}
Treatment * Timepoint	2	1.26	5.33×10^{-1}	2	1.5	4.72×10^{-1}
Geometric Mean of PcUBC11, PcVHA-A, and PcUBA1						
Treatment	2	0.01	9.93×10^{-1}	2	0.36	8.35×10^{-1}
Timepoint	1	0.36	5.49×10^{-1}	1	0	9.99×10^{-1}
Treatment * Timepoint	2	1.16	5.59×10^{-1}	2	1.27	5.30×10^{-1}

Table 4. Summary of analysis of deviance of generalized linear mixed models fit to xylem reference gene qRT-PCR expression data. Asterisks (*) indicate interactions between factors. All genes were fit to the following formula: transcript abundance ~ time point * treatment, family = Gamma (link = log).

	G. clavigera inoculation			MPB attack		
	df	**χ^2**	***p***	**df**	**χ^2**	***p***
PcUbiquitin-activating enzyme 1 (PcUBA1)						
Treatment	2	3.16	2.06×10^{-1}	2	1.69	4.29×10^{-1}
Timepoint	1	13.06	$\mathbf{3.01 \times 10^{-4}}$	1	0.06	8.11×10^{-1}
Treatment * Timepoint	2	2.09	3.52×10^{-1}	2	0.21	9.01×10^{-1}
PcUbiquitin-conjugating enzyme 11 (PcUBC11)						
Treatment	2	3.25	1.97×10^{-1}	2	1.08	5.81×10^{-1}
Timepoint	1	10.54	$\mathbf{1.17 \times 10^{-3}}$	1	0.01	9.23×10^{-1}
Treatment * Timepoint	2	4.22	1.21×10^{-1}	2	0.34	8.44×10^{-1}
PcVacuolar ATP synthase subunit A (PcVHA-A)						
Treatment	2	3.02	2.21×10^{-1}	2	1.75	4.16×10^{-1}
Timepoint	1	12.42	$\mathbf{4.25 \times 10^{-4}}$	1	0.18	6.70×10^{-1}
Treatment * Timepoint	2	2.91	2.33×10^{-1}	2	0.22	8.94×10^{-1}
Arithmetic Mean of PcUBA1 and PcVHA-A						
Treatment	2	3.08	2.15×10^{-1}	2	1.75	4.17×10^{-1}
Timepoint	1	12.57	$\mathbf{3.92 \times 10^{-4}}$	1	0.13	7.14×10^{-1}
Treatment * Timepoint	2	2.66	2.64×10^{-1}	2	0.21	8.99×10^{-1}
Arithmetic Mean of PcUBA1 and PcUBC11						
Treatment	2	2.31	3.15×10^{-1}	2	1.23	5.40×10^{-1}
Timepoint	1	12.31	$\mathbf{4.50 \times 10^{-4}}$	1	0.02	8.97×10^{-1}
Treatment * Timepoint	2	3.24	1.98×10^{-1}	2	0.32	8.53×10^{-1}
Arithmetic Mean of PcUBC11 and PcVHA-A						
Treatment	2	2.47	2.90×10^{-1}	2	1.32	5.16×10^{-1}
Timepoint	1	12.22	$\mathbf{4.72 \times 10^{-4}}$	1	0.06	8.14×10^{-1}
Treatment * Timepoint	2	3.28	1.94×10^{-1}	2	0.29	8.64×10^{-1}
Geometric Mean of PcUBA1 and PcVHA-A						
Treatment	2	3.12	2.10×10^{-1}	2	1.74	4.19×10^{-1}
Timepoint	1	12.72	$\mathbf{3.61 \times 10^{-4}}$	1	0.11	7.44×10^{-1}

Treatment * Timepoint	2	2.48	2.90×10^{-1}	2	0.21	8.98×10^{-1}
Geometric Mean of PcUBA1 and PcUBC11						
Treatment	2	2.66	2.64×10^{-1}	2	1.42	4.92×10^{-1}
Timepoint	1	12.68	$\mathbf{3.70 \times 10^{-4}}$	1	0.03	8.73×10^{-1}
Treatment * Timepoint	2	2.75	2.53×10^{-1}	2	0.26	8.76×10^{-1}
Geometric Mean of PcUBC11 and PcVHA-A						
Treatment	2	2.57	2.76×10^{-1}	2	1.42	4.91×10^{-1}
Timepoint	1	12.33	$\mathbf{4.46 \times 10^{-4}}$	1	0.07	7.86×10^{-1}
Treatment * Timepoint	2	3.23	1.99×10^{-1}	2	0.24	8.85×10^{-1}
Arithmetic Mean of PcUBC11, PcVHA-A, and PcUBA1						
Treatment	2	2.57	2.77×10^{-1}	2	1.39	4.99×10^{-1}
Timepoint	1	12.28	$\mathbf{4.58 \times 10^{-4}}$	1	0.06	8.14×10^{-1}
Treatment * Timepoint	2	3.12	2.10×10^{-1}	2	0.28	8.69×10^{-1}
Geometric Mean of PcUBC11, PcVHA-A, and PcUBA1						
Treatment	2	2.8	2.47×10^{-1}	2	1.53	4.64×10^{-1}
Timepoint	1	12.57	$\mathbf{3.92 \times 10^{-4}}$	1	0.06	8.01×10^{-1}
Treatment * Timepoint	2	2.81	2.46×10^{-1}	2	0.24	8.89×10^{-1}